8-2020

Analysis of Interdunal Wetlands and Ecosystem Dynamics using UAS and OBIA in Ludington State Park, Michigan

Claire Gilbert
Western Michigan University, claire.gilbert1223@gmail.com

Analysis of Interdunal Wetlands and Ecosystem Dynamics using UAS and OBIA in Ludington State Park, Michigan

by
Claire Gilbert

A thesis submitted to the Graduate College
in partial fulfillment of the requirements
for the degree of Master of Science
Geography
Western Michigan University
August 2020

Thesis Committee:

Adam J. Mathews, Ph.D., Chair
Kathleen Baker, Ph.D.
Tiffany Schriever, Ph.D.

Analysis of Interdunal Wetlands and Ecosystem Dynamics using UAS and OBIA in Ludington State Park, Michigan

Claire Gilbert, M.S.

Western Michigan University, 2020

The Great Lakes sand dunes are the world's largest freshwater dune complex. There is a functional relationship between coastal wetlands and freshwater sand dune, referred to as interdunal wetlands. Interdunal wetland systems are highly dynamic and change dramatically seasonally and annually. Using geographic information systems (GIS) and unoccupied aerial systems (UAS), this thesis project is focused on understanding the spatial distribution of sparse and dense vegetation, and abiotic influence such as distance to coast, slope, and aspect influence interdunal wetland stability within a Great Lakes shoreline dune system. Object-based image analysis (OBIA) classification results extracted meaningful vegetation densities of growth and loss and wetland growth and loss features for spatial analysis. Vegetation growth is more predominant in west and south portions of wetlands and is more stable, while the north and east portions of wetland tend to expand.

ACKNOWLEDGMENTS

There are countless of incredible people who guided me on this endeavor and deserve appreciation and gratitude for their efforts. I would like to extend my sincerest gratitude to Dr. Adam Mathews and Dr. Kathleen Baker for their guidance and direction over the years. Words can truly not explain how thankful I am to have had the opportunity to work alongside you; it has been an unequivocal privilege.

To Dr. Mathews, the experience and skills gained from your mentorship has made me and twice the person and academic that I would have been without your constant support. Thank you for introducing me to the world of remote sensing, joining me for fieldwork, enriching my academic ambitions, your advice, and constantly finding new opportunities for me to explore that will benefit my skill development and future career.

To Dr. Baker, thank you for setting the bar high for my expectations in research and future ventures and I promise I will hold both myself accountable to this high level of excellence as I go forward in life. For the past 5 years, you have placed confidence in my capabilities, sparked my enthusiasm and appreciation for GIS, and have taught me so much more than the boundaries of GIS.

I would also like to thank Dr. Tiffany Schriever for her assistance as a committee member and allowing me to be involved in a portion of her research. A special thanks to Greg Anderson, for the advice, laughs, and encourage you have provided me while working together.

And, as always, many thanks to my family and friends who constantly provide support, encouragement, and challenge me to do my best in everything I do.

Claire Gilbert

TABLE OF CONTENTS

Table of Contents – continued

Table of Contents – continued

LIST OF TABLES

LIST OF FIGURES

List of Figures - continued

INTRODUCTION

Wetlands are defined as areas of land experiencing water at or near the surface of the ground for a portion of the year (Gray, 2000). These areas define habitats for specific organisms adapted for variable water systems, soil types, and wildlife communities (EPA, 2004). Wetlands, more importantly, play a role in providing complex ecosystem services including structures for biodiversity and wildlife habitat; functions of water purification, carbon sequestration, nutrient retention, flood prevention, soil development, and climate change mitigation; processes for nutrient cycling, primary productivity, and nitrogen removal; food production, fibers, fish and crustaceans; and uses for recreation and human well-being (LaPage, 2011; Ying-zi et al., 2008). LePage (2011) explains that wetlands are inextricably linked to human health, and ecological impacts such as climate change and infrastructure growth are affecting the quality and quantity of benefits humans depend upon.

Wetland functions and successional stages largely influence ecological health and adaptability of dune ecosystems. The mechanisms and processes of a particular complex of dunes determine species composition due to sand transportation, the burial of pioneer vegetation, establishment of stabilizing vegetation, and soil profiles (Johnson & Miyanishi, 2008). Wetlands systems situated in coastal dune systems, referred to as interdunal wetlands, along the Great Lakes are of particular interest in this research. The Great Lakes sand dunes are the world's largest freshwater dune complex. There is a functional relationship between coastal wetlands and freshwater sand dune.

Interdunal wetlands form in troughs of the Great Lake sand dunes and are sources of great biodiversity and plays a critical role in productivity and the hydrologic cycle. Using geographic information systems (GIS) and unoccupied aerial systems (UAS), this thesis research maps the spatial distribution of sparse and dense vegetation and to understand how the patterns influence dune regression and growth, and wetland stability within a Great Lakes shoreline dune system. This project investigates a wetland system within a Lake Michigan dune system that experiences varying stability of vegetation and wetland shape and size. The ecosystem services wetlands provide to wildlife and human well-being can be considerably affected by prevailing environmental conditions and climate change. The immediate surroundings of interdunal wetlands such as vegetation densities, and influences of wind disturbance, dune slopes, and distance to the shoreline were analyzed to understand the whole interdunal wetland complex.

This thesis is concerned with vegetation densities, sparse and dense, and their relationship with wetlands and dune dynamics at Ludington State Park (LSP) (see Figure 1). The sparse vegetation being classified contains herbaceous plants such as grasses and low-lying shrubs, while the dense vegetation is classified by tree canopy cover. By classifying the vegetation densities, an opportunity for a more detailed analysis of plant-environment, plant-plant, and plant-animal interactions among interdunal wetlands is possible. Characterizing the existing sparse vegetation as a pioneer or stabilizing species for dune succession provides information on interdunal successional stages, and more importantly, the overall biodiversity and productivity of interdunal wetland. This project analyzes areas of significant dune and wetland movement, and clusters of sparse or dense vegetation to understand how each wetland and the immediate surrounding of vegetation densities interact.

Remote sensing advancements have increased as a result of UAS enhancements. Now, the research capabilities have substantially increased with UAS lower cost and higher accessibility of digital cameras that allow for higher spatial and temporal aerial imagery than satellite imagery. (Mathews, 2015; Hardin & Jensen, 2011). Standard UAS used for small-scale research are fixed or rotary-wing aircrafts manufactured with lightweight material and adaptive programming that meets the needs of consistent flight paths, limited battery power, and Federal Aviation Administration (FAA) regulations. Hardin & Jensen (2011) outline data analysis opportunities using UAS for environmental research; with commercial image processing software, researchers can process large UAS datasets into large-scale products and maps for further data analysis. UAS imagery allows research to obtain specific spectral information of the targeted environment, with high spatial resolution of 3 cm.

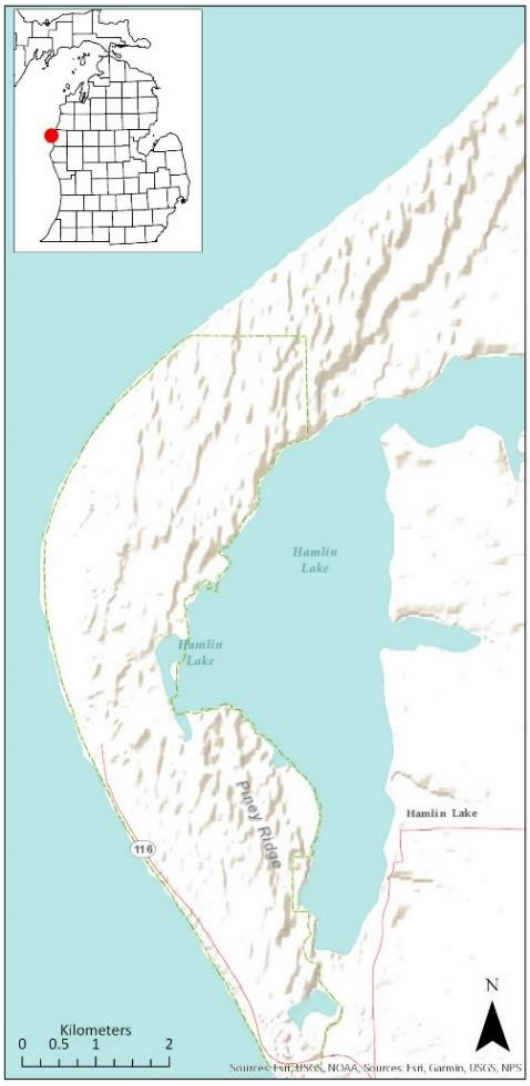

Figure 1. Ludington State Park reference map.

Research Questions

The importance of examining the relationship of latitudinal gradients among vegetation structures and habitat conditions of interdunal wetlands has been recognized by researchers and Great Lakes programs and agencies (Albert, 2003; EPA, 2004; Albert et al., 2005). There is limited research on interdunal wetlands, specifically, areas with freshwater resources. Research is needed for the identification of vegetation types, a better understanding of complex species interactions, and sustainable management practices of interdunal wetlands. In summary, there is

a need for a better understanding of wetland communities. More specifically, the following research questions are addressed at Ludington State Park in Ludington, Michigan:

1. What are the spatial distributions of sparse and dense vegetation found in these ecosystems?
    a. What are the abiotic differences such as slope, aspect, and distance to Lake Michigan for the spatial distributions of sparse and dense vegetation trends?
2. How dynamic is the stability of wetlands in this ecosystem?
    a. What is the annual and monthly stability wetland or growth or reduction of this ecosystem?
    b. What are the most prevalent variables for dune and wetland stability?
        i. How does sparse or dense vegetation influence the stability of wetlands?

Research Justification

Michigan Sea Grant – tracking biodiversity in Lake Michigan's interdunal wetlands

An ongoing case study in interdunal wetlands along the east coast of Lake Michigan includes documenting invertebrate and amphibian species populations throughout the areas of interest from 2017 to 2019 (see Figure 2). The interdunal wetland research project is funded by a Michigan Sea Grant of nearly $200,000 overseen by Tiffany Schriever, Ph.D., an assistant professor of biology at Western Michigan University (WMU). The research group is examining the relationship between macroinvertebrate community structure and habitat conditions, including the spatial and temporal patterns of amphibians, the taxonomic and functional structure of macroinvertebrate assemblages, and landscape-level genetic patterns in coastal aquatic insects. The objective of this research group is to access biodiversity throughout Lake Michigan's coastal wetlands on the leeward side of dune ridges. This research project is the first of its kind in

Michigan. The research areas begin with Indiana Dunes State Park located on the southern shore of Lake Michigan; the following areas increase latitudinally on the east coast, starting with Warren Dunes State Park, followed by Saugatuck Harbor Natural Area, LSP, and Sleeping Bear Dunes.

This thesis project allows for more robust understandings of interdunal wetlands and supplement the ongoing case study funded by a Michigan Sea Grant through application of remote sensing techniques to understand the ecological interaction between associated vegetation densities found within interdunal wetlands. While the WMU Department of Biological Sciences is looking at species types and populations of macroinvertebrates and amphibians at multiple locations, this research project focuses on LSP one of the five interdunal wetland ecosystems currently being studied by Schriever's lab situated along the eastern coast of Lake Michigan. Potentially, future research implements the significant findings derived from remote sensing analyses for this site to the remaining interdunal wetlands ecosystem being studied.

Figure 2. Interdunal wetlands on the Lake Michigan coast.

Overall reasoning

Remote sensing applications and additional research methods are interdisciplinary, joining WMU Geography and Biological Sciences graduate programs. LePage (2011) states that wetland managers need to be educated in all aspects of wetland science, including ecology, geography, geology, engineering, socio-political, and economic components to be successful in wetland restoration and enhancement. Remote sensing applications allows the biology research

lab to investigate the importance of vegetation densities within interdunal wetlands further. The research finding from both departments can educate shoreline environmental managers on how to make sustainable decisions for these unique wetland types. Additionally, the prominent spatial pattern of vegetation densities found in this reach can lead to a further understanding of high biodiversity locations, where more invertebrates and amphibians are likely to be found, and where extensive sampling should take place.

BACKGROUND

Introduction

Due to limited research specifically focused on interdunal wetlands, a multidisciplinary approach concerning separate studies of dune systems, wetland systems, and remote sensing techniques is needed. While ecological knowledge is necessary background, there is a greater focus in the literature review on remote sensing techniques and their application to the ecology of dune areas. The research presented in the following literature review outlines what is currently feasible in terms of vegetation classification and species habitat assessment. Background research related to dune and wetland systems illustrates the dynamics of all interdunal wetlands.

The phenology of associated vegetation is an important consideration when acquiring ground reference data and aerial imagery. Additionally, anthropogenic activities are changing wetland stability and signifies that an interdisciplinary environmental management approach is needed. The recent research advances in remote sensing applications allow for improved techniques to monitor highly dynamic systems. The presented opportunities for lidar-imagery fusion allows better surveying techniques of interdunal wetlands. The ideal approach for analyzing the ecological uniqueness of these concentrated and dynamic systems is through object-based image analysis (OBIA) techniques.

Dune Profiles and Wetland Systems

To fully understand the complexity of interdunal wetlands, knowledge of landscape ecology and eco-services is necessary. Landscape ecology is a broad term to describe and investigate "spatial structure, interaction, coordination function and process of the landscape

composed by many different ecosystems" (Wang et al., 2008, p. 164). Moreover, it stresses spatial ecology, scale, patterns, and dynamics to maintain ecological stability. Wetland landscapes are ecosystem mosaics of heterogeneous characteristics of aquatic and terraneous transition belts, with abundant biotic and abiotic resources (Wang et al., 2008). Interdunal wetlands are naturally rare and dynamic coastal ecosystems that fluctuate seasonally and cyclically (Lightfoot et al., 2020).

As mentioned previously, wetland ecosystem services provide structures, functions, processes, goods, and uses for the landscape. Wetland Management is concerned with implementing practices and policies to protect and enhance ecological services (LePage, 2011). Furthermore, research regarding the landscape ecology of wetlands relies heavily on geospatial tools and techniques (e.g., remote sensing, GIS, GPS). Researchers can collect, interpret, and analyze spatial data more efficiently and with more accuracy through the advancements of remote sensing platforms.

For accurate vegetation classification in interdunal wetland systems, it is crucial to understand the dynamics and processes of wetlands and dune systems. Previous research on wetland functions along environmental gradients provides insight into expected surface characteristics. Wetlands are areas of transition between aquatic and terrestrial ecosystems that provide a niche for specially adapted species. Brinson (1993) classifies wetlands by type using the relationships among precipitation, groundwater, and overland flow as determinant variables. There are distinct water movements that affect the variation of sediments throughout the wetland, including inflow and outflow rates, elemental content such as nitrogen and phosphate, and water sources.

Albert et al. (2005) outlined a hydrogeomorphic classification system for Great Lakes Coastal Wetlands. Within this framework, Ludington State Park's interdunal wetlands are classified as either Open or Protected Lacustrine Systems of shoreline or embayment potentially encompassing nontidal Palustrine systems (see Figure 3 and 4). Open Lacustrine systems are lake controlled, possessing littoral sediment, sand-bar development, that pose limitations for organic sediment accumulation, vegetation expansion, and little to moderate diversity of macroinvertebrates. Nearshore processes of wave climate affect dune profiles and can range from steep to shallow slopes. Due to prevailing winds, vegetation development is relatively unabundant within 100 meters from the shoreline.

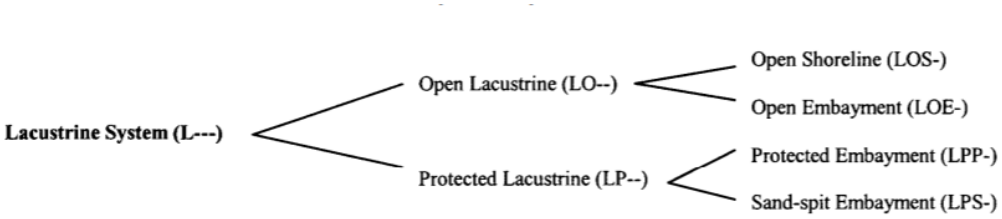

Figure 3. Hydromorphic classification for Great Lakes wetlands (Source: Albert et al., 2005).

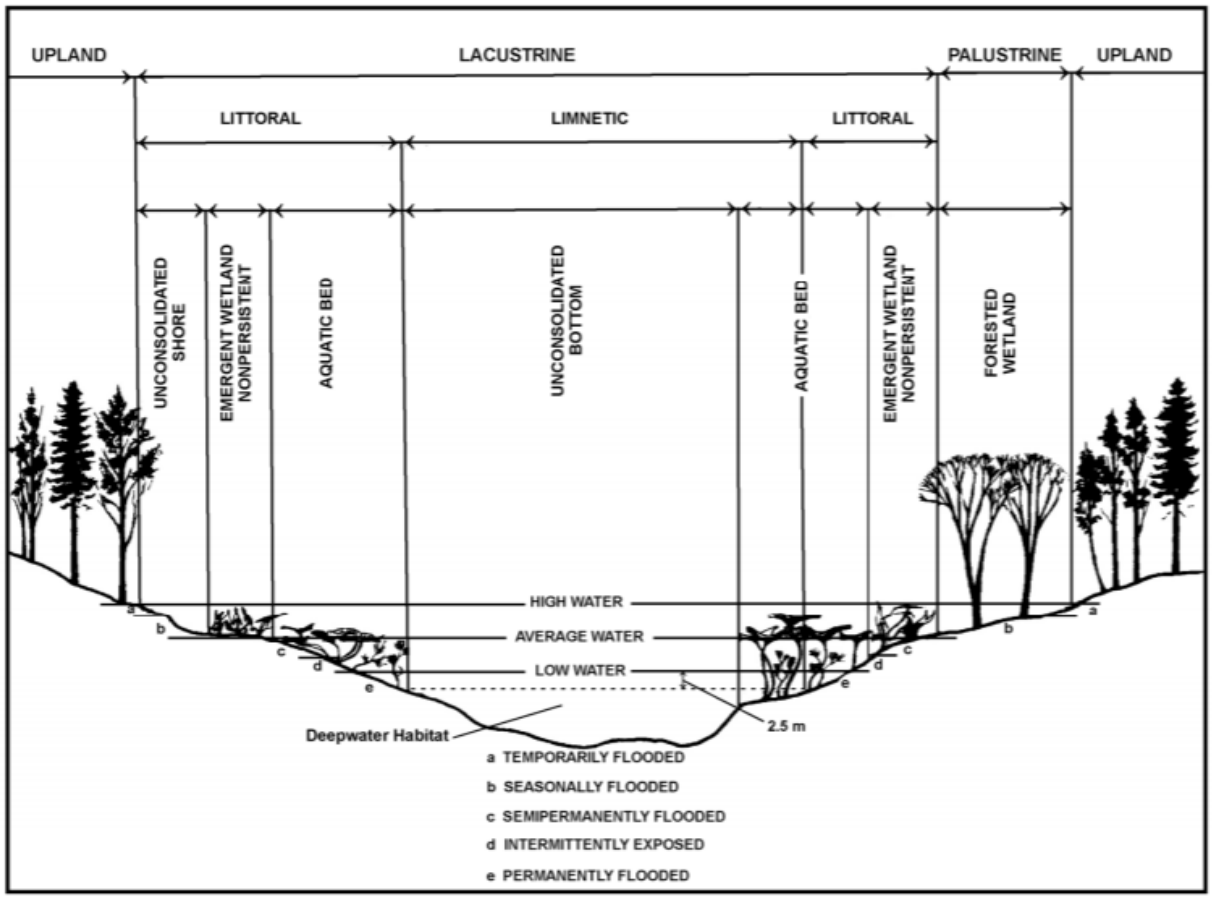

Figure 4. Wetland Lacustrine System classification showing the proximity and potential of Palustrine forested wetland (Source: Federal Geographic Data Committee, 2013).

Lakes and watersheds control the formation of Protected Lacustrine Systems. They are identified with sand-spit, offshore bar, or till-enclosed bays of protection with increased organic sediment accumulation and diversity of aquatic and surrounding terraneous vegetation (Albert et al. 2005). These wetlands have high diversity in submerged and emergent vegetation and high diversity in macroinvertebrates. However, protected embayment and sand-spit wetlands are quite different; in contrast, embayment systems have extensive vegetation development around till indentations, sand-spit wetlands form on gentle slopes, and have sparse vegetation due to moderate organic sediment accumulation (Albert et al. 2005).

Following Albert et al. (2005) research, Kost et al. (2007) further defined interdunal wetland communities for Michigan Natural Feature Inventory (MNFI). As noted by the Federal

Geographic Data Committee (FGDC) (2013), "Islands of Palustrine wetland may lie within the boundaries of the Lacustrine System." In this case, our research of interdunal wetlands are classified as Palustrine within the Lacustrine System (see Figure 5 and 6). These wetlands are a branch down from Palustrine marshes that are located in the depressions of open embayment or the middle of sand-split dune ridges (refer to Figure 4) (Kost et al., 2007). Additionally, the depressions and wetlands were likely influenced by wind creating bluff blowouts or historic river channels. The water-level fluctuations of Lake Michigan influence the creation of linear depressions inside the upland foredune and foredune along the shoreline (Kost et al., 2007). Further, upland dunes and wetlands are less influenced lake's water-level.

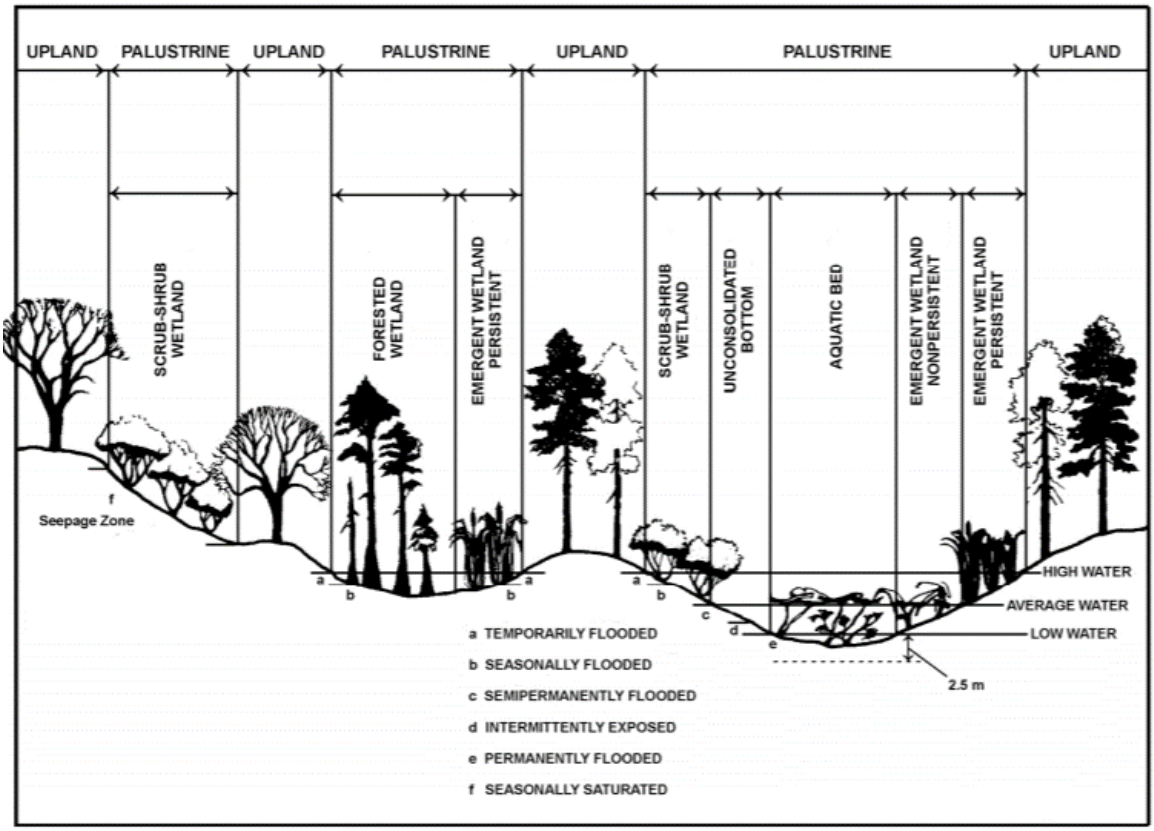

Figure 5. Wetland palustrine system classification of temporal flooding (Source: Federal Geographic Data Committee, 2013).

Figure 6. Wetland in open embayment dune (Source: Frazier, 2017).

Interdunal wetlands are dominated by herbaceous vegetation; rush, sedge, and shrubs that are adapted for fluctuating water tables and saturated sand and wetland water with neutral to moderately alkaline. The wetlands unconsolidated bottom and shore substrate contains dead plant tissue, promoting rooted vascular submergent plants, floating vascular plants, and diversity of invertebrate fauna (see Figure 7).

Figure 7. Interdunal wetland with rooted vascular plants and surrounding vegetation (Source: Cohen et al., 2020).

Dune systems are highly dynamic and change dramatically seasonally and annually (Delgado-Fernandez et al., 2009). Natural processes of dune growth and regression develop over several types of land cover within a wetland, providing a unique niche. Successional stages of dune vegetation fluctuate throughout the dune system. Dune succession is a 'complex gradient of changing environmental constraints' that directly effects vegetation growth, survival, and reproduction (Lichter, 1998). Strong prevailing winds, high insolation, sand mobility, high rates of evaporation, low availability of nitrogen and phosphorus, and beach use have substantial effects on early successional plant communities (Lichter, 1998).

Plants participate in the stabilization and development of dune systems, by continuing primary, secondary, and tertiary growth. When vegetation becomes the driver for dune stabilization and growth due to root structure and catchment for mobile sand. Furthermore, as distance increases from the shoreline, dune age and community structure become more developed because plants participate in stabilization and development of dune systems as environmental constraints lessen.

These transition areas typically have numerous functional variations, but researchers often focus on a single environmental factor when classifying these areas. Additional factors related to the relationships of all the previously mentioned aspects, as well as soil composition, determine the wetness of the wetland, and thus the plant species complexes that are present in any specific interdunal wetland (Albert et al., 2005; FGDC, 2013; Moor, 2017). Additionally, climatic conditions such as precipitation and temperature that determine root growth and root mass and dispersal are also necessary.

Root growth requires sufficient biochemical resources and species-specific soil temperatures within an acceptable range. Phenology shows a correlation between springtime warming, soil temperature, and new root and shoot growth (Clarke et al., 2015). Previous testing of shoot growth confirms that soil temperatures are the driving factors for branching, canopy development, and leaf size. However, sandy soils of interdunal wetlands pose a challenge for accurate phenology predictions within the system due to fluctuating coastal dune conditions. It is challenging to monitor anthropomorphic beach use; human activities range from little disturbance to severe disturbances, but without a doubt, the accumulation of activities alters the morphology of dune profiles. Furthermore, more anthropomorphic disruptions and pressures impair the maturation of plant communities to a greater extent (Straford and Rooney, 2017).

Applications of Remote Sensing to Wetlands Research

There is a need to monitor wetland ecosystems, and field surveys provide the most detailed information on specific small-scale research sites. However, the impracticality of fieldwork in cost and time on a large swath of land directs researchers to the use of remotely sensed images. Remote sensing provides satellite, aircraft imagery, and data on larger scales with less time and money invested. With the analysis of wetland imagery, there are several implications related to inconsistent levels of accuracy. High temporal and spatial resolution imagery is ideal for accurate assessment of wetlands; however, there might be challenges with the availability of imagery data sources, especially given the high correlation between dune environments and clouds that potentially obscure the ground view for any given time of day or season. As shown in Table 2, many researchers use satellite imagery for ecological analysis of wetlands increasingly paired with supplemental imagery most recently provided by unoccupied aerial systems (UAS).

One challenge of wetland monitoring is greater energy absorption due to higher variable moisture content of sand that affects camera sensors. Additionally, land cover is often not homogeneous given the gradients of vegetation diversity and developments, fluctuations of reflectance values and noise from vegetation interspersed with sand, and dynamic energy reflection of varying water levels and movements. To gather accurate imagery for subsequent analyses, integration of passive and active sensors, and ground-reference data is recommended to improve accuracy (Gallant et al., 2015). Ground-reference data has substantially higher spatial and spectral resolution compared to large image datasets (Jensen, 2005). Reference data may be acquired by field spectroradiometers or UAS imagery that is used to compare and augment the results of the remote sensing-derived thematic map. It is typical in a project to integrate imagery

from different spatial and multispectral resolutions to allow intensive manual interpretation of wetlands (Hardin et al., 2018).

Typical remote sensing of wetlands involves image segmentation, the collection of supervised training sample points, and a subsequent supervised classification (Jensen, 2005). Jensen (2005) explains supervised classification as subdividing the imagery into spectral regions based on preciously field-collected training samples, while unsupervised classification clusters pixels by the natural grouping based only on homogeneous spectral data. Both supervised and unsupervised classification allows for a comparison of ground-truth spectral signatures and clusters of signatures to develop optimal spectral response patterns (Klemas, n.d.).

Improvement of mapping temporary wetlands can be supplemented with recurrent Landsat imagery. Dvorett et al. (2016) utilized Landsat 5 and 7 images covering a study area of 1300 km^2 along the Cimarron River in Central Oklahoma for early, peak, and post-growing seasons were collected, and training pixels in five land-cover classes were selected. Before image classification, training pixels are selected by the image analyst that represent homogenous sites for targeted land-cover types (Jensen, 2005). Training pixels from multiple images can increase the accuracy of seasonal variability in spectral signatures. However, it may be more challenging to determine the extent of interdunal wetlands given the variable inundation patterns and irregular periods of vegetation development

2.3.1 Lidar applications

Active sensors such as light detection and ranging (lidar) systems are equipped with a laser scanner emitting near-infrared pulses, a GPS receiver, and an inertial measurement unit (IMU) to capture 3D measurements, stored as point clouds, with associated latitude, longitude, and elevation coordinate data (Ellis and Mathews, 2018). An understanding of morphological

and hydrological parameters is needed before digital elevation models (DEM) can be generated from lidar data. More locational attributes can be created from DEMs and digital surface models (DSM), including slope angle, slope aspect, plan curvature, profile curvature, tangent curvature, flow direction, flow accumulation, specific catchment areas, and steady-state topographic wetness index. Soil landscapes have direct relationships with soil properties, even excluding moisture and terrain attributes. Once a digital terrain map is completed, it is possible to predict future landscape changes based on spatial patterns of terrain attributes (Bou Keir et al., 2010).

The fusion of satellite imagery and lidar-derived DEM data is often used to delineate and characterize wetlands (Chasmer et al., 2013; Rapinel et al., 2017). Rapinel et al. (2017) used lidar imagery fusion to extracts data delineating potential, current, efficient, and lost wetlands by acquiring lidar during early spring to avoid vegetation foliage shadows, a common issue of satellite images, and integrate satellite imagery with spectral signatures during the growing season.

Corbane et al. (2015) evaluate remote sensing techniques for natural habitats and report the accurate wetland vegetation classification is difficult without lidar. Traditional methods using mid-to near-infrared bands have limited spectral returns due to soil saturation; moreover, the researchers recommend the integrated use of ancillary data, lidar, and hyperspectral imagery (see Table 1 for sensor suitability for wetland distinction). It should be noted here that this study used DEMs and DSMs with imagery for classification. The main difference is that the active sensor used for DEM generation records the ground elevation, while a passive sensor used for the DSM generation records the elevation of everything on the surface. Meaning, DSM supplies elevation of vegetation structures and DEMs supply elevation underneath the vegetation.

Table 1. Sensor suitability for mapping natural habitats in wetlands (adapted from Corbane et al., 2015).

Sensors and Resolution	**Capability**
Low spatial and high temporal (MODIS, AVHRR)	N/A
Medium to high spatial and temporal (Landsat, IRS, SPOT)	Seasonal imagery allows mapping the spatial extent of submerged wetland and some vegetation species, and functional wetland types
Very high spatial (IKONOS, GeoEye, WorldView-2)	Detection of riparian vegetation species, shallow, and submerged vegetation
Hyperspectral (HyMap, CASI, Hyperion)	Distinction between aquatic macrophyte species
Laser Scanning (LiDAR)	In combination with multispectral imagery High precision LiDAR-derived digital terrain map is used to build the relationship between wetland vegetation species and associated ground elevation. May enhance the understanding of the characteristics of different wetland vegetation species
Active Microwave Sensor	N/A

Unoccupied Aerial Systems (UAS) and photogrammetry

UAS can be used to map and monitor vegetation with onboard digital cameras at a very high spatial resolution. UAS provides accessibility and control for assessing environmental targets (Aber et al., 2010). UAS equipped with a digital camera capable of sensing various bands in the electromagnetic spectrum. The images collected from the aircraft can be instantaneously reviewed and processed by the remote pilot., Ground control points (GCPs) with known reference system coordinates are used to georeference the imagery (Aber et al., 2010). Georeferenced images from multiple perspectives are implemented in Structure from Motion-Multi-View Stereo (SfM-MVS) programs to create a three-dimensional scene. SfM, a computer vision technique, stems from traditional photogrammetry and has been utilized extensively for surveying in recent years (Carrivick et al., 2016). SfM-MVS generates three-dimensional (3D) point cloud data using overlapping aerial photographs captured by the UAS.

There are six essential steps to produce SfM-MVS an orthomosaic and point cloud data including feature detection, keypoint correspondence, keypoint filtering, Structure from Motion, scaling, and georeferencing via GCPs, and MVS (Carrivick et al., 2016). This process, in its entirety, is commonly referred to simply as SfM. Carrivick et al. (2016) explain the following steps to obtain dense point cloud data. Feature detection matches images together based on feature points and identifies keypoints of invariant object characteristics that can be assigned to multiple imagers with different viewpoints. Keypoint correspondence and filtering involves an algorithm to describe features and orientation within the image, and then filter out the errors of specific images. The SfM step utilized a modified bundler algorithm (Snavely et al., 2003) to create a sparse point cloud on an arbitrary coordination system. After SfM, the sparse cloud data is coupled with an absolute reference system based on the GCPs. MVS is the next step that eliminates redundant images that have the same image clusters and produces a 3D reconstruction of the scene in dense point cloud datasets. The point cloud data can be applied in a GIS and preform an interpolation conversion to a digital surface model (DSM). Additionally, the DSM can aid object-based image classification by providing an additional band of information (Mathews, 2015).

Remote Sensing of Dune Dynamics

Lidar techniques are best for the study of both short-term and long-term coastal sand dynamics (Klemas, 2011), and combining digital terrain models with hyperspectral data often improves emergent benthic vegetation analysis (Klemas, 2011). Recent advancements in lidar techniques now offer valuable 10 cm vertical accuracy per one square meter of highly dynamic sedimentary surroundings, i.e., coastal and dune systems. An example of this application is a

study by Arbogast et al. (2009), where the researchers use lidar-derived point clouds to estimate sand volume estimation.

Remote sensing analysis of coastal dunes requires extensive knowledge at varying temporal and spatial scales, particularly to the dune system. To address this issue, Delgado-Fernandez et al. (2009) used three mounted digital SLR cameras to obtain time-lapse imagery over two months over their study area of the Greenwich Dunes on Prince Edward Island National Park. Once the imagery is processed, it is critical to calibrate initial moisture content reading by averaging red, green, and blue band pixels to obtain a greyscale grid to normalize the sand's moisture brightness values. As noted earlier, comparisons of night and day images indicate that dunes are more dynamic during the night.

Object-based Remote Sensing for Vegetation Classification

Object-based image analysis (OBIA) can be used for automated extraction of various land cover layers. Vegetation classification is possible using OBIA by applying specific parameters to delineate individual plant species. OBIA is a preferred method due to its range of applicability and ease of data fusion (Ellis and Mathews, 2018). The primary objective of OBIA is to extract meaningful objects, for further evaluation (Blaschke, 2010), often utilizing high spatial resolution imagery. Analysis at the object-scale requires higher resolution imagery for accurate delineation for a regionalized group of pixels. Moreover, high resolution is also required for small vegetated populations within interdunal wetlands. High-resolution products allow image segments to be broken into categories of point-based, edge-based, region-based, and data layers whereby a combination of these can be adopted for better classification. Once the classification is complete, vector feature classes are created.

WorldView-2 satellite imagery is a standard product that is used for vegetation mapping and phenology type based on the object-based approach. A multi-resolution segmentation algorithm can generate general homogeneous objects with set parameters of scale, shape, and compactness. Multi-seasonal imagery significantly improves vegetation classification, while lidar is useful for the identification of vegetation functional types. High temporal data helps identify phenology dynamics in various vegetation types (Yan et al., 2018). Additionally, wetland plant functional types can be classified by C3 grasses; C3 forbs; C4 and C3 reeds; C4 short grasses; emergent aquatic macrophytes; and floating and submerged aquatic macrophytes. Cluster analysis of the functional types can then be implemented in image segmentation. Plant functional type classification can be utilized in OBIA based on the distinct groupings of spectral signatures (Dronova et al., 2012).

Ellis and Mathews (2018) conducted vegetation delineation of urban tree canopy change in Oklahoma City through high spatial resolution object-based image analysis (OBIA). OBIA methods used NAIP imagery, lidar, and lidar data fusion performing within 82-96% accuracy in calculating vegetation change between 2006 and 2013. Another application of lidar data collection uses a 50% overlap of scan lines to reduce canopy shadows and to allow the sampling of each side of treetops. Chasmer et al. (2016) employ lidar data to compare aerial photograph mosaics and Alberta Ground Cover Classification (AGCC) to delineate and improve peatland and wetland classification. Vegetation classification is established first to show land cover transition boundaries of forest to wetlands.

To successfully classify vegetation types, a fusion of DEMs and/or DSMs, texture of physical landscapes, topographic data, and various spectral data is recommended (Chasmer et al., 2014; Rapinel et al., 2017; Xie et al., 2008; see Table 2 for lidar data fusion examples). Chasmer

et al. (2014) and Knight et al. (2013) use a decision-tree land-cover classification utilizing multispectral resolutions, textures, and hierarchical classification procedures. Hierarchical classification can better delineate sub-layers of vegetation based on an appropriate spatial resolution for each land cover type.

Table 2. Image classification approaches in similar research.

Publication	Classification/Methods	Platform	Data Source	Results
Chasmer et al., 2014	Decision-Tree Fusion Classification	Geomatica OrthoEngine	Aerial imagery and LiDAR	OA = ~ 91%
Chasmer et al., 2016	LiDAR-based unsupervised classification	n/a	LiDAR	Errors of commission 32% Errors of omission 6%
Chabout et al., 2018	Object-based image analysis; machine learning classifier	ENVI 5.4 QGIS	High-Resolution UAS imagery	Above-water features OA = 89-92% Submerged features OA= 74-84%
Dronova et al., 2014	Object-based image analysis; machine learning classifier	eCognition	Landsat 5 TM	OA = 85-90%
Dronova et al., 2016	Object-based image analysis; machine learning classifier	Weka 3.6.5 ArcGIS 10	Worldview-1 and QuickBird	OA = 94.3%
Dvorett et al., 2016	Decision-tree classification	R ENVI 5.2	Landsat 5 Landsat 7 LiDAR NAIP imagery	Kappa = 96%
Ellis et al., 2018	Object-based image classification	Monteverdi	LiDAR and NAIP imagery	OA = 88-89%
Knight et al., 2013	Decision-Tree classification	See5	NAIP imagery LiDAR	OA = 93% and 77%
Im et al., 2013	Object-based image analysis; machine learning classifier	Definiens	LiDAR	OA = > 90%
Rapinel et al., 2017	unsupervised	ArcGIS	LiDAR Historical aerial photos	OA = 88-90%
Yan et al., 2018	Object-based image analysis;	eCognition	WorldView-2	OA = 82.3-91.1%

Object-based Change Detection

OBIA can be used for regular and rapid interdunal wetland dynamics assessment. Lightfoot et al. (2020) describe a study to evaluate the change-detection of coastal ecosystems using OBIA. Post-classification change assessment involves the comparison of wetland shape and area from different dates of data acquisition and object classification. One advance of post-classification change detection is the supply information for the direction of change and transitional "from-to" classes. The methodology consists of calculating the mean proportion of the total area of targeted wetland feature classes; calculating the transitional from-to classes mean proportion of total area, and calculating the total area change of each wetland feature class. Furthermore, a comparison map with wetlands, densities of vegetation, and sand classes with attributed change proportions of the total area give insight to the nature, significance, and spatial distribution and patterns of interdunal wetland ecosystems (Lightfoot et al., 2020).

DATA AND METHODS

Overview

To address the research objectives, this research applied an object-based image classification approach using remotely sensed data captured on August 13, 2018, September 9, 2019, and October 18, 2019. For 2018 aerial imagery, dense vegetation, sand, and wetlands were classified, while 2019 aerial imagery obtained by UAS was classified into sparse (herbaceous) vegetation, dense (canopy cover) vegetation, sand, and wetlands. Accurate spatial and temporal scales were critical for accurate vegetation classification, and fieldwork was an iterative process for vegetation spectral signature measurement and observation (Jensen, 2005; Klemas, n.d.). Remote sensing techniques include preprocessing, OBIA (i.e. segmentation, attribution, and classification), and accuracy assessment. Data collection and analysis take on an empirical approach, constructing a model for vegetation and wetland relationships. Physically based numerical models involve the independent variables categorized from fieldwork observations and aerial imagery.

Study Area

The area of interest is in the Great Lakes Region on the west coast of the lower peninsula of Michigan. Ludington State Park (LSP) in Ludington, Michigan (Mason County) is situated between Lake Michigan and Hamlin Lake with over a mile stretch of Big Sable River running through (refer to Figure 1). The study portion falls inside the Stony Creek-Frontal Lake Michigan watershed within the Pere Marquette-White watershed basin. The natural processes of

wetland formation in this area occur when water-levels drop, establishing swales and depression between the inland dunes and newly created coastal foredune, then pooling up when water levels rise (Kost et al., 2007).

LSP provides an especially unique ecosystem to examine, encompassing several environments such as dune, beach, wetland, marsh, and forest. LSP contains the largest area of interdunal wetlands, in the world, and provides important feeding areas for migrating shorebirds, waterfowl, and songbirds (USDA – Forest Service, 2006). The park contains woody vegetation, including Juniper, Jack Pine, and Hemlock, and is home to endangered Pitcher's Thistle and Piping Plover shorebirds. Dominant plants in the area can withstand sand burial and water-level fluctuations. Larger and deeper open wetlands are associated with surrounding shrubs and grass and often have emergent plants in shallow water (Kost et al., 2007). Readers are referred to Appendix A for a list of plants found in Michigan interdunal wetlands.

Data and Data Processing

Imagery and lidar from July 25, 2018 were collected from the National Agriculture Imagery Program (NAIP) downloaded via the USGS Earth Explorer. High-resolution NAIP imagery (Figure 8), in this case 4-band (B, G, R, NIR) 1-meter spatial resolution, enables assessment of the fluctuations of vegetation over different time intervals. As for the 2019 imagery, two UAS flight campaigns took place in September and October. LSP is a large park in terms of land area (0.369 km^2) and requires extensive sampling to cover the size and variability of geographic processes and for statistical analysis. The targeted variables that need to be characterized on-site include the extent of vegetation and temporary wetlands, dense vegetation of canopy cover, and sparse herbaceous vegetation groupings. These variables were tested to find

a relationship between wetland shape and size, distance from the shore, and surrounding vegetation.

Figure 8. NAIP orthomosaic of study area, 2018 (1 m spatial resolution).

Fieldwork

Fieldwork was performed at LSP once on September 9 (2019a) and October 18 (2019b) (Figures 9 and 10 respectively). A quadcopter UAS, specifically the DJI Mavic Pro 2, collected nadir aerial imagery on-site. The author served as the remote pilot (licensed by the Federal Aviation Administration) for data collection purposes adhering to flying restrictions under Part 107, the Western Michigan University Drone Policy (request approved), and Michigan State Parks/Department of Natural Resources (use permit approved). The UAS was equipped with integrated Hasselblad RGB optical sensor. The UAS had five preprogrammed flight plans, using the Pix4Dcapture smartphone application, that acquired images throughout autonomous flight. Due to technical issues, only three of the five plans were able to be executed for 2019a in September. While 2019b covered a larger area, 1.064km^2, the study area was reduced to the area covered by 2019a. In an interdunal wetland environment, there is little flight path planning needed to avoid obstacles. The UAS surveyed at a flying height of 390 ft above the ground surface flying in both east-west and north-south directions (i.e. double-grid pattern) with a 75% forward (or front) overlap between images and 70% side overlap between successive flight lines. Given the extent of the area of interest and need for accurate georectification, 20 Propeller AeroPoint GCPs were dispersed throughout the study area. Due to areal coverage differences, only 7 out of 20 GCPs were observed in 2019a, while 2019b data acquisition observed 17.

Photogrammetry

Before SfM-MVS photogrammetric processing, each image was inspected for blur and lighting issues. Poor images were removed. Further, UAS-collected GNSS coordinates were cleared from the image metadata to rely solely on ground survey for georectification. This indirect georeferencing method was preferred because the AeroPoint GNSS accuracies (both

horizontal and vertical) are higher than the onboard UAS GNSS. SfM-MVS image matching was then conducted using Pix4Dmapper, which automatically detects keypoints within the area of interest that had several images matched to it, and then keypoint match correspondence with other images was carried out. The arbitrary coordinates from the sparse point cloud were transformed into the Michigan Central State Plane (ft) coordinate system using the known locations recorded by the Propeller AeroPoints (post-processed via the Propeller cloud; differentially corrected to 5.7 mm horizontal error and 3.81 mm vertical error on average) visible within the collected aerial photos.

The 2019a dataset incorporated all 741 images collected. The 2019b dataset utilized 1,151 of the 1,207 images collected. The sparse point cloud generating SfM algorithm was applied followed by the MVS algorithm to create a dense point cloud (example provided with Figure 11). The dense point cloud was converted to a digital surface model (DSM) raster and used to find the slope angle, slope aspect, plan curvature, profile curvature, tangent curvature, flow direction, flow accumulation throughout LSP. Moreover, digital photogrammetric processing provided high spatial resolution (3 cm) georeferenced orthomosaics for 2019a and 2019b for OBIA (Figures 9 and 10) as well as DSMs (Figure 12) for further analysis. SfM-MVS orthomosiacs contain RGB bands from the original images. In addition, the DSMs were stacked in the orthomosaics as a fourth band to aid OBIA processing.

Figure 9. Orthomosaic of study area created from UAS imagery, 2019a (3 cm spatial resolution).

Figure 10. Orthomosaic of study area created from UAS imagery, 2019b (3 cm spatial resolution).

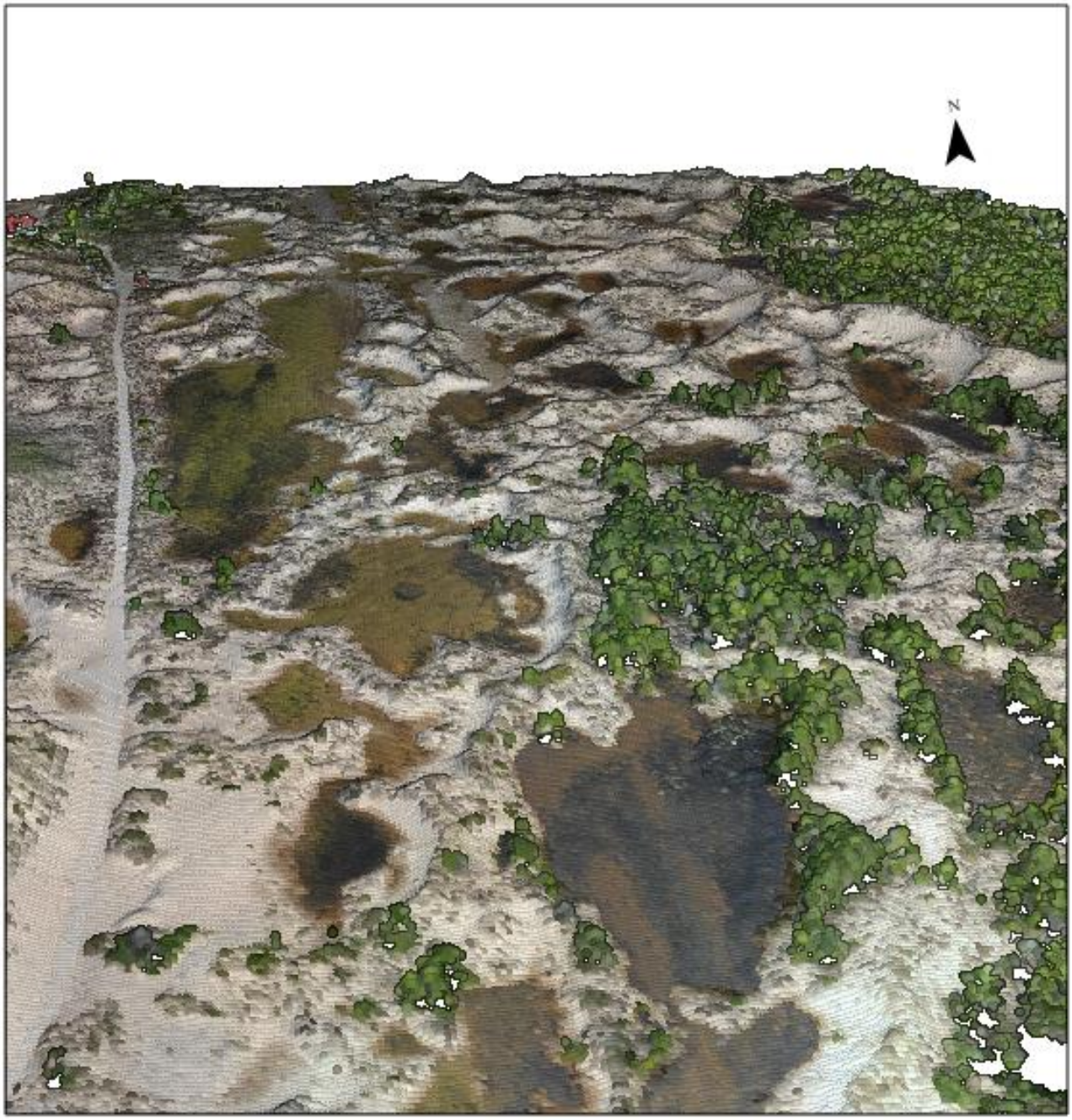

Figure 11. SfM-MVS dense point cloud for 2019a.

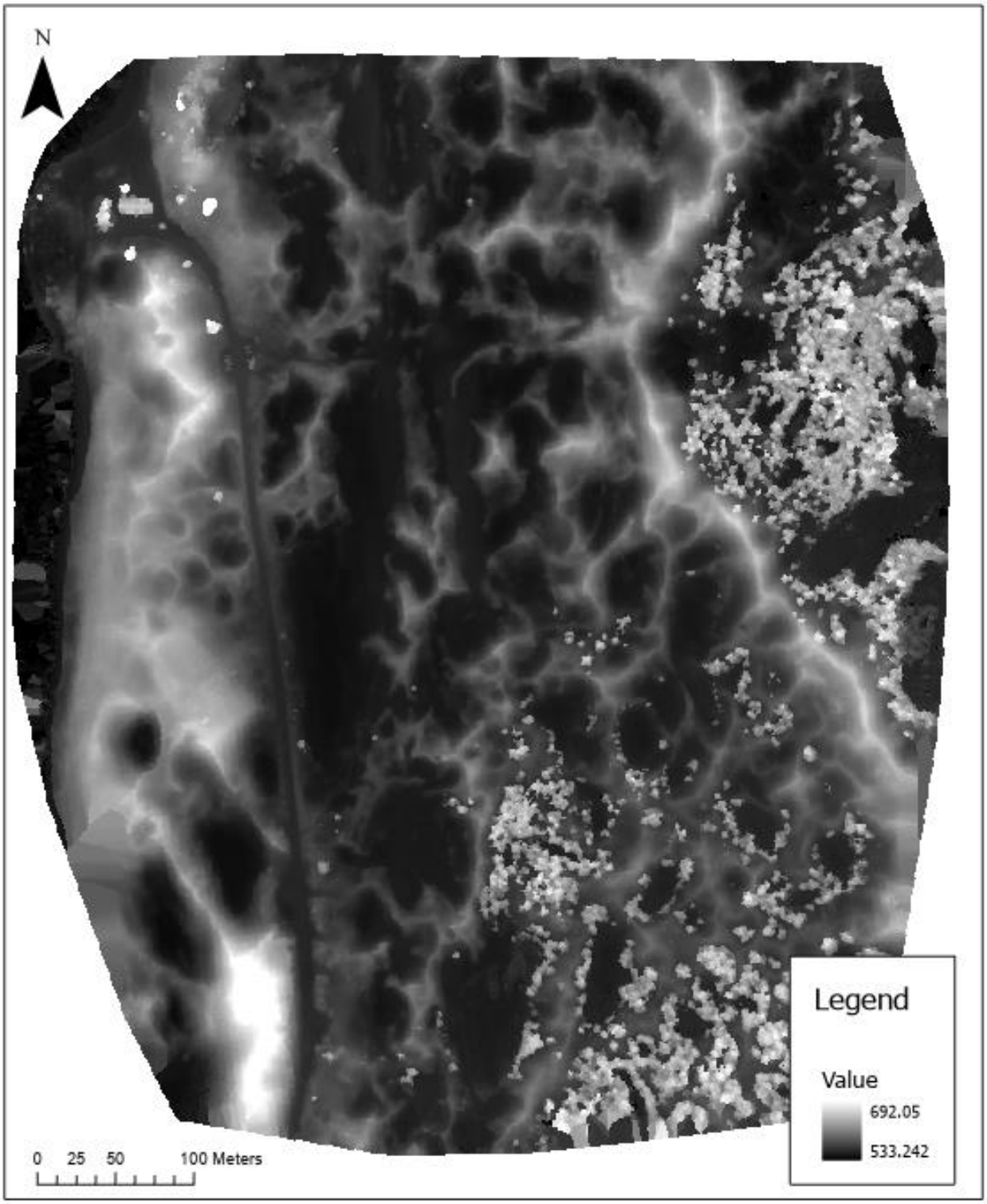

Figure 12. SfM-MVS derived digital surface model for 2019a.

Object-based Image Analysis (OBIA) of Ludington State Park land cover types

ArcGIS Pro's Image Classification Wizard was used to streamline OBIA and to configure the supervised classification schema (i.e. image segments or objects were grouped using a supervised approach). Before classification, all orthomosaics went through a series of mean shift segmentation iterations to identify the optimal parameters of spectral and spatial detail as well as segment size of pixel groupings. The final parameters for segmentation used 18.5 spectral, 17 spatial, and a minimum segment size of 50 pixels. Segments were grouped using the National Land Cover Dataset (NLCD) classification schema. The final land cover classes include water, barren (sand or soil), herbaceous (sparse vegetation), and canopy cover (dense vegetation). The water classification delineated the wetland extent of the water edge to either sand or vegetation objects. The sparse vegetation delineation grouped clusters of grass, rush, sedge, and shrubs of at least 50 pixels. Additionally, the imagery and DSM fusion for OBIA was very useful and produced a high accuracy of dense vegetation delineation and wetland water edge.

After running the mean shift segmentation using the optimal parameters, the training sample manager prompted a manual selection of various segment size, pure pixels, and mixed pixels. Two hundred training samples were placed into each class: water, barren, sparse vegetation, and dense vegetation (sparse and dense vegetation were combined for 2018) using the orthomosaics and segmented raster. The training samples were used in support vector machine classifier for OBIA. The next step is the reclassifier tool, and this allowed inaccurate pixel groupings reassignment to the correct grid code.

An accuracy assessment was performed by creating 500 stratified random points to test the ground truth against the final OBIA map. Once the pixel groupings reached the highest accuracy, the rasters were converted to vector shapefiles, features. The accuracy assessments for

2018 and both 2019 datasets indicated that manual digitization was necessary (see Tables 3-5) , and more than 40 hours of work corrected the shape of all feature classes; wetlands, sparse vegetation, and dense vegetation (see Figures 13 and 14)

Table 3. Land cover accuracy assessment of 2018 NAIP imagery.

	Class Value	Vegetation	Barren	Water	Total	User Accuracy	Kappa
NLCD	**Water**	14	92	16	122	0.131147541	0
	Barren	0	167	0	167	1	0
	Vegetation	66	47	0	113	0.584070796	0
	Total	80	306	16	402	0	0
	Producer Accuracy	0.825	0.545751634	1	0	0.619402985	0
	Kappa	0	0	0	0	0	0.381911366

Table 4. Land cover accuracy assessment of 2019a UAS imagery.

	Class Value	Canopy Cover	Herbaceous	Water	Barren	Total	User Accuracy	Kappa
NLCD	**Water**	17	22	71	30	140	0.507142857	0
	Barren	0	20	10	168	198	0.848484848	0
	Canopy Cover	43	7	1	4	55	0.781818182	0
	Herbaceous	2	58	16	32	108	0.537037037	0
	Total	62	107	98	234	501	0	0
	Producer Accuracy	0.693548387	0.542056075	0.724489796	0.717948718	0	0.678642715	0
	Kappa	0	0	0	0	0	0	0.541655

Table 5. Land cover accuracy assessment of 2019b UAS imagery.

	Class Value	Water	Barren	Canopy Cover	Herbaceous	Total	User Accuracy	Kappa
NLCD	**Water**	30	5	24	22	81	0.37037037	0
	Barren	4	69	5	71	149	0.463087248	0
	Canopy Cover	0	0	61	1	62	0.983870968	0
	Herbaceous	4	5	18	57	84	0.678571429	0
	Total	38	79	108	151	376	0	0
	Producer Accuracy	0.789473684	0.873417722	0.564814815	0.377483444	0	0.57712766	0
	Kappa	0	0	0	0	0	0	0.442038

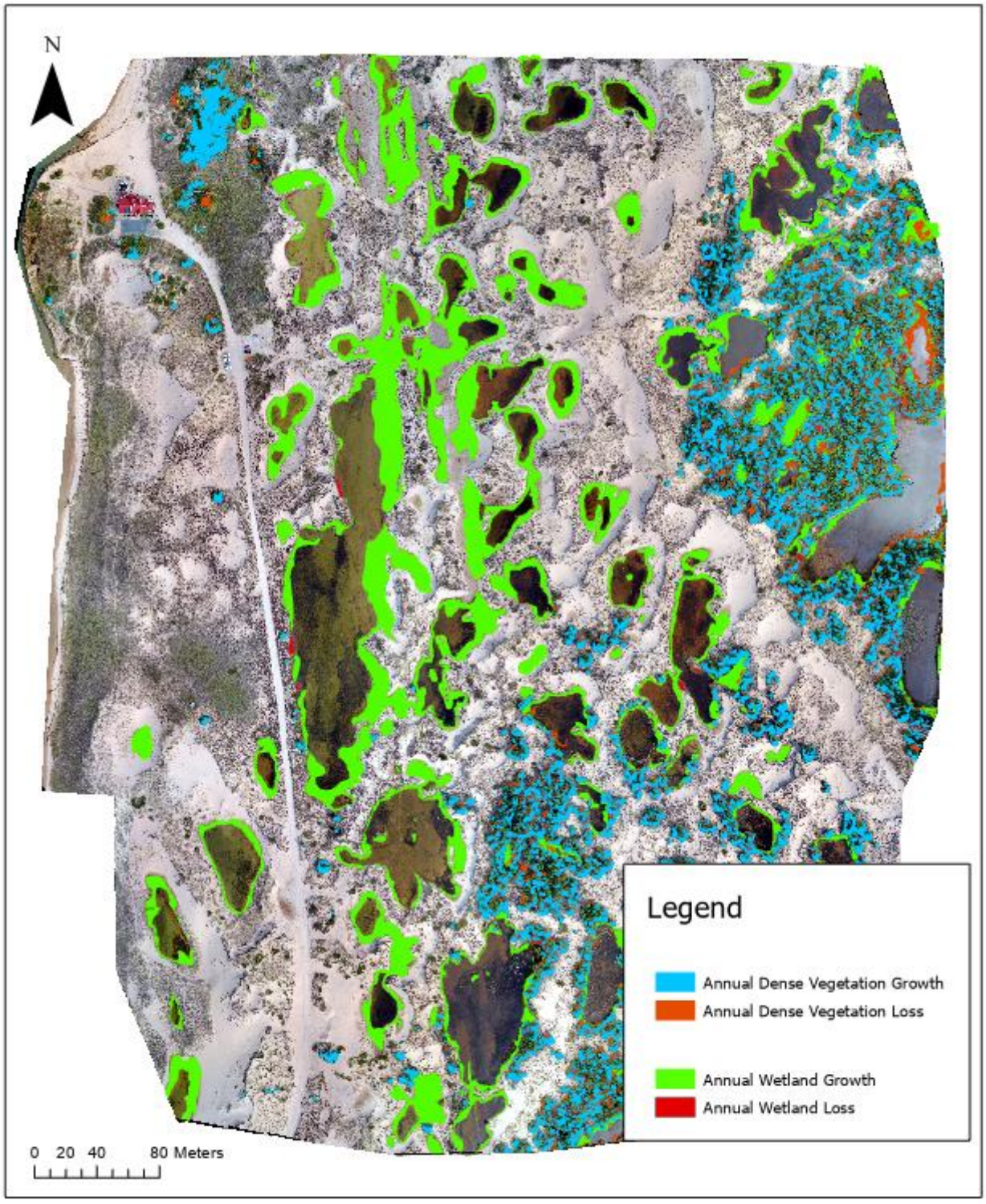

Figure 13. Wetland and vegetation growth and loss features between 2018 and 2019a.

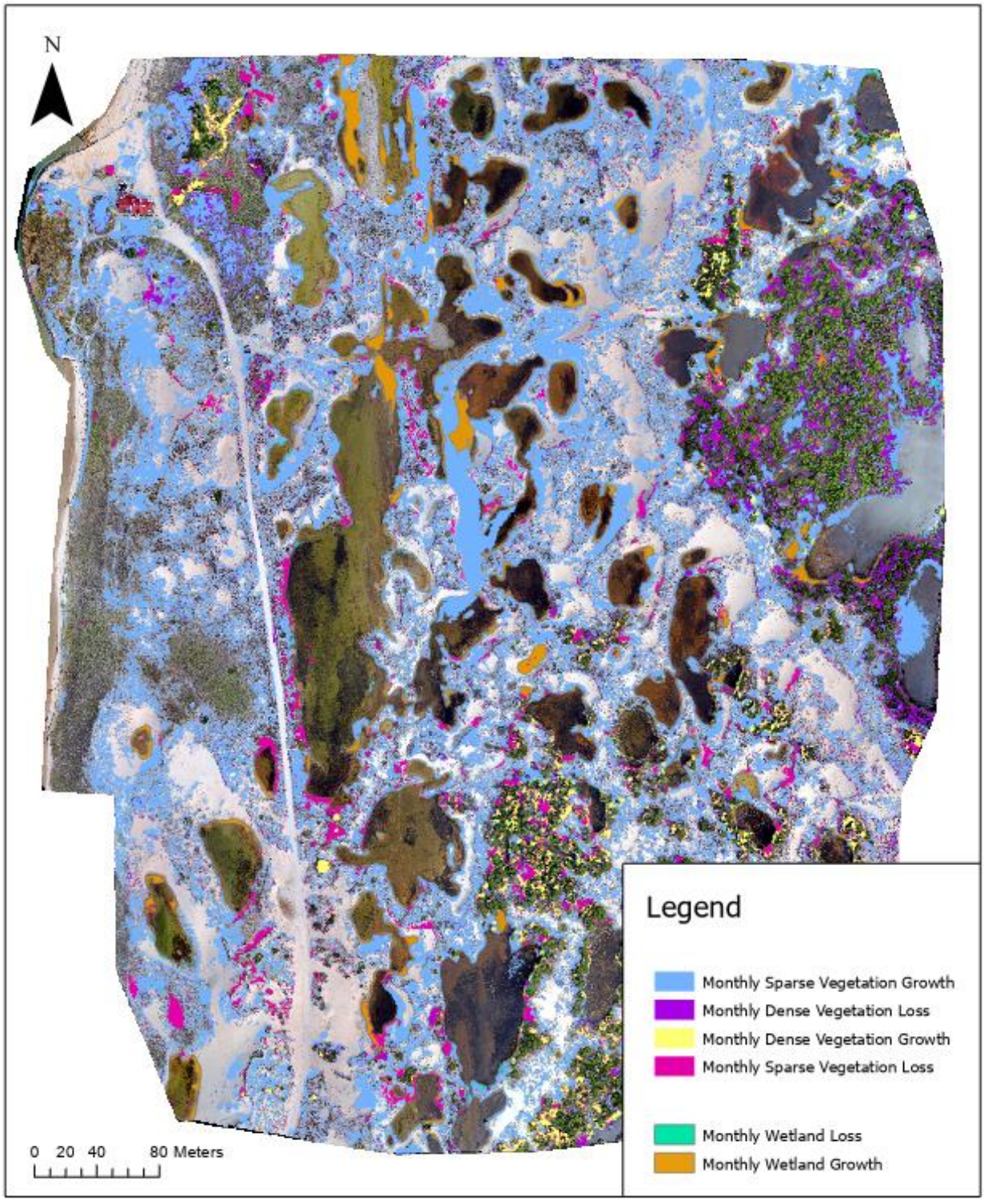

Figure 14. Wetland and vegetation growth and loss features between 2019a and 2019b.

Spatial Analysis

The main objective of this project is to have a better understanding of spatial patterns and tendencies within interdunal wetland ecosystems. A series of overlay tools and zonal statistics was performed for 2018, 2019a, and 2019b for additional attributes for statistical testing and feature association. The Symmetrical Difference overlay tool was used to locate areas of loss and growth in sparse and dense vegetation and wetlands. Using the symmetrical difference tool, the sparse and dense vegetation and wetland features from 2018, 2019a, and 2019b were used to create new change detection features where there is no overlap. The change detection features represent month and annual changes of vegetation densities (sparse and dense) and wetland. Polygon area and perimeter length define geometry attributes and the shape metrics of features. After, polygons of growth and loss were separated, and geometry attributes were added to the features. Calculation of geometry attributes were added to each feature class. Annual change between 2018 and 2019a and monthly change between 2019a and 2019b define the stability of the ecosystem.

The proximity of surrounding features is needed to understand the spatial arrangement of the ecosystem. Vegetation within a 10-meter Euclidean distance buffer of wetlands are considered directly proximal to a specific wetland. To note, the 10-meter buffer was decided based on the ongoing Michigan Sea Grant study, for a preliminary and broad understanding on surrounding wetland vegetation. Using merged feature classes of 2018, 2019a, and 2019b wetlands, a 10-meter and 5-meter buffer were created around every wetland feature. Additionally, the buffers were segmented into 4 cardinal direction quadrants. The buffers were subdivided using equal area parameter to ensure the quadrant areas are normally distributed. An additional parameter was made for the degree of angle from which to segment the quadrants are

as follows: north is 135 – 45; east is 45 – 315; south is 315 – 225; and west is 225 – 135 (Figure 15). The quadrants allow for an assumption of predominant slope aspect leading up to the wetland. To clarify, the north quadrant exhibits southern facing slopes, east quadrants have west facing slopes, etc. Slope and aspect are of particular interest because of vegetation growth and sun insolation. Slope and aspect irregularities and variation alter radiation, temperature, evaporation, and wind speed causing difference of plant composition and formation (Millington et al., 2011). The aspect tool was used on 2018, and both 2019 DSMs that underwent zonal statistics to get the average slope direction for each buffer quadrant.

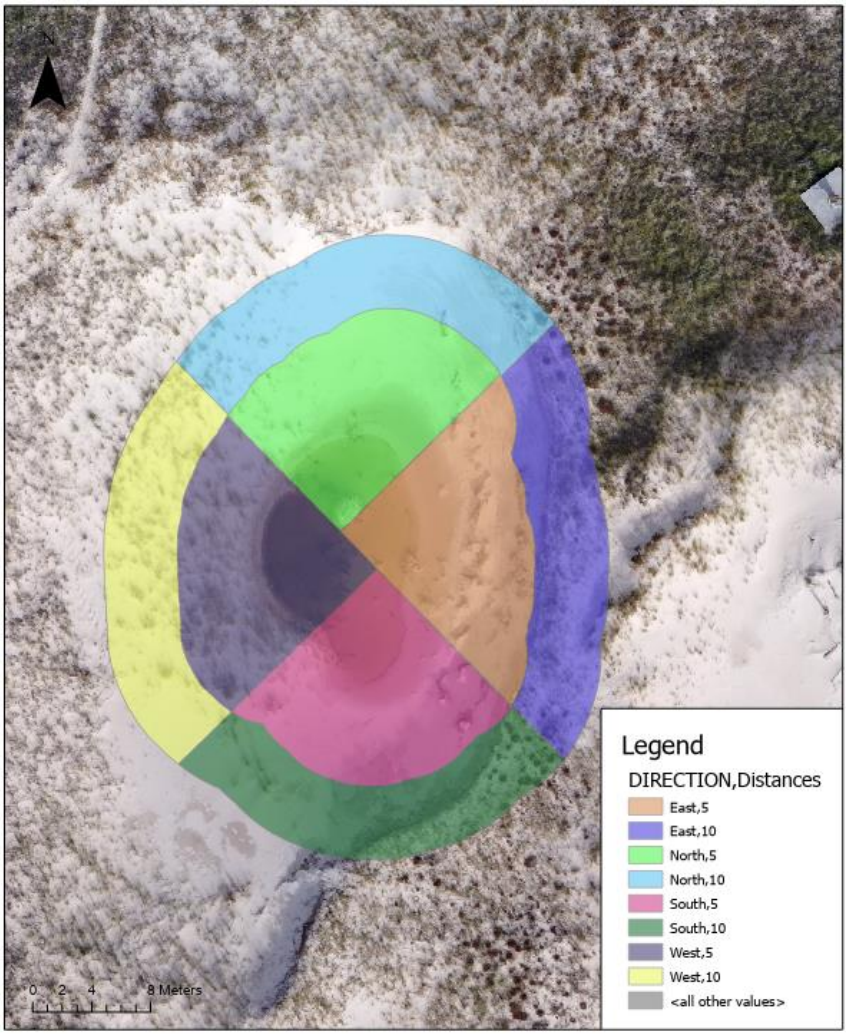

Figure 15. Wetland buffer cardinal direction quadrants for a single wetland.

Distance to lakeshore/coastline can influence how wetland stability is affected by lake effects such as wind, tides, and distance. A distance raster was generated with the Euclidean Distance tool from the shoreline. To gather information on dune gradients and associated wetland change, slope was calculated on 2018 DEM and both 2019 DSMs. DSMs derived from the point clouds were used to create percent rise of dune slopes. To make sure the assumption was correct on quadrant slope directions, the Aspect tool was used to get the direction of Slope that was converted into a feature class (Figure 16).

To get individual statistics for the amount of vegetation and wetland change within a specific aspect, the aspect polygons were then updated to the 10 and 5-meter buffers. To get each individual cardinal quadrants statistics of slope, predominant aspect, and distance to the shoreline, the zonal statistics tool was performed on each of the wetland 10 and 5-meter buffers. Tabulate Intersection tool calculated how much area and the percentage of coverage by sparse and dense vegetation and wetland within 10 meters of the specific wetland (see Table 6). After all attributes and statistics of features were calculated, the dataset included area and percentages in the buffer of a wetland of 2018 and both 2019 wetlands, sparse vegetation growth and loss, annual and monthly dense vegetation growth and loss, distance to coast, mean slope, and aspect.

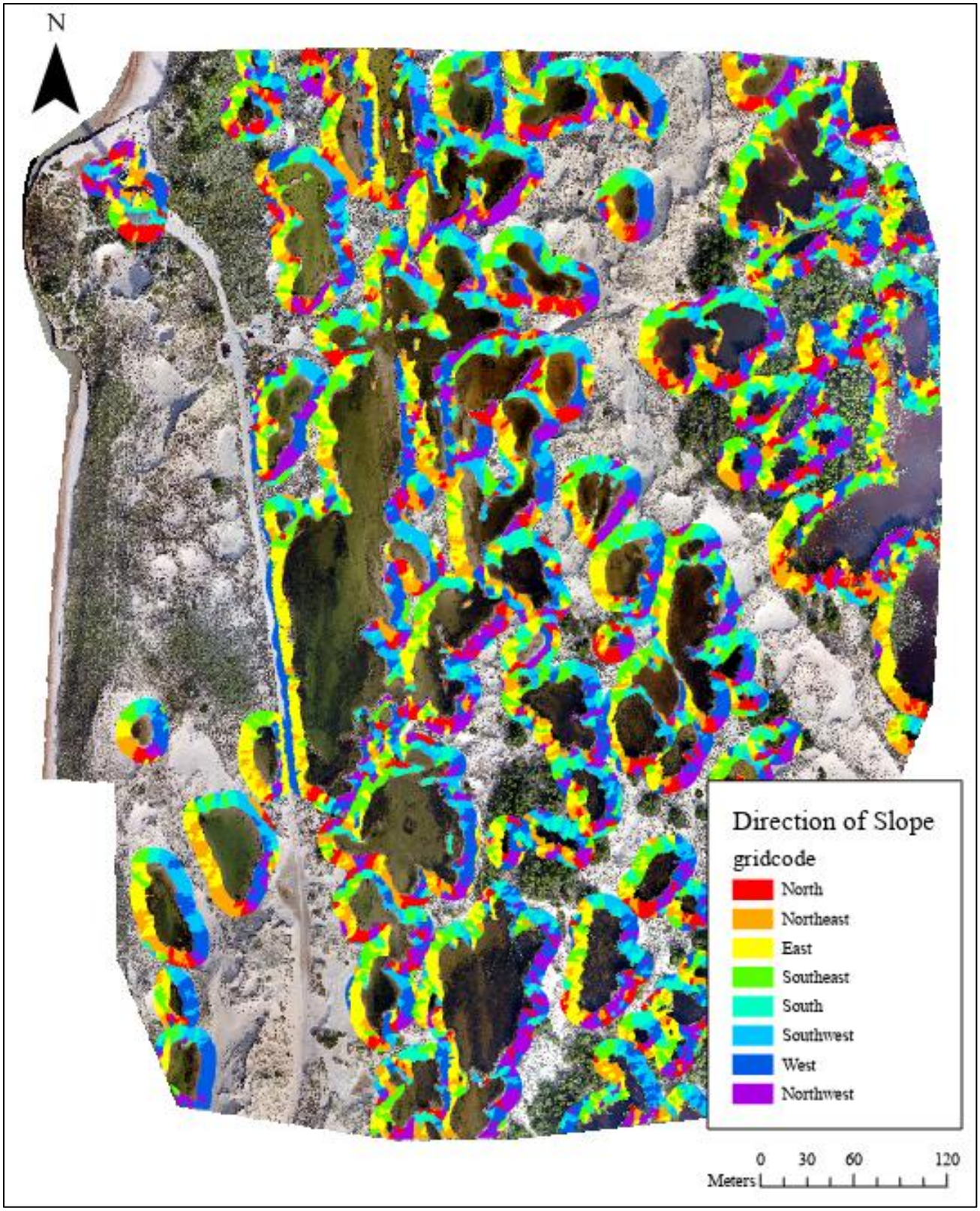

Figure 16. Aspect of slope within the 10-meter buffer around wetland features in LSP.

Table 6. Partial results from tabulate intersection.

OBJECTID	DIRECTION	WGM_AREA	WGM_PERCENTAGE	DGM_AR	DGM_PERCENTAGE	DLM_AREA	DLM_PERCENTAGE
57	South	1.34624	0.233035	114.010463	19.7353	25.183833	4.359341
22	West	37.388388	5.087828	107.583984	14.640074	57.434474	7.815708
23	East	24.833569	3.379371	92.12969	12.537079	45.476065	6.188418
189	South	65.676938	2.736239	89.12085	3.712961	33.178524	1.382287
61	South	9.450424	1.02511	86.67248	9.401571	24.629232	2.671591
82	West	54.86545	16.759772	84.149575	25.705206	2.837107	0.866652
67	East	59.402975	2.340512	83.853783	3.303888	75.291192	2.966517
58	West	11.171944	1.933868	81.520485	14.111226	21.059148	3.645346
191	East	128.592369	5.357429	81.433625	3.392696	41.945004	1.747517
327	West	14.386813	5.002346	80.465525	27.978149	36.63931	12.739618
115	West	3.047196	0.68122	80.056132	17.897057	15.116838	3.379465
37	South	15.05007	2.37018	77.91722	12.270898	40.934413	6.446611
59	East	40.294254	6.974968	73.473273	12.718283	17.467343	3.023611
68	North	99.731027	3.929467	73.000032	2.876249	48.006609	1.891491
565	South	59.316019	3.308061	69.283502	3.863949	26.561419	1.481333
104	North	25.254218	4.969322	67.807671	13.342649	16.19213	3.186157
402	South	9.356409	2.065448	67.413534	14.881689	26.419512	5.832167
434	West	11.171903	2.98697	66.752359	17.847207	8.573479	2.292243
433	South	1.353715	0.361937	66.619586	17.811784	4.290892	1.147237
567	East	132.265173	7.376449	65.133758	3.63252	27.377388	1.526841

Changed Area and Wetland Stability

Wetlands

Within the study area, 108 wetlands in 2019a covering 74,577.6 m^2 with a range of 2.78 m^2 to 14,610.04 m^2, while 2019b had 98 wetlands covering 82,501.33m^2 with a range of 6.93 m^2 to 22,960.92 m^2. In 2018, OBIA was used to extract 86 wetlands covering a total area of 52,521.76 m^2 with sizes ranging from 22.23 m^2 to 8,748.17 m^2. It is necessary to note that the spatial resolution limitation of 2018 imagery resulted in the inability to extract (and, thus, analyze) shallower interdunal wetlands where the water boundary line was not delineated from OBIA . From 2018 to 2019a, wetland area expanded by 22,055.85 m^2 (1.42% increase); the smallest wetland delineated in 2018 was 22.23m^2, while 2019a delineation was as small as 2.78m^2. From 2019a to 2019b, wetland area expanded by 7,923.72 m^2 (1.11% increase).

Between 2018 to 2019b, wetland area expanded by 29,979.57 m^2 or an increase of 1.32% (Table 7).

The growth of wetlands spatially adhered to a parallel directionality compared to the shorelines. The closer the wetlands are to the shore the more potential they have to be highly dynamic. There are more stabilizing factors the farther away the wetlands are to the shoreline. Wetland expansion occurs in areas with relatively low slopes. For example, the largest wetland (Figure 17) in 2019 experienced the amalgamation of seven adjacent wetlands. In the central northeast there is an area of low-lying slopes (2 – 10 degrees) exhibiting a tendency toward wetland expansion around that area.

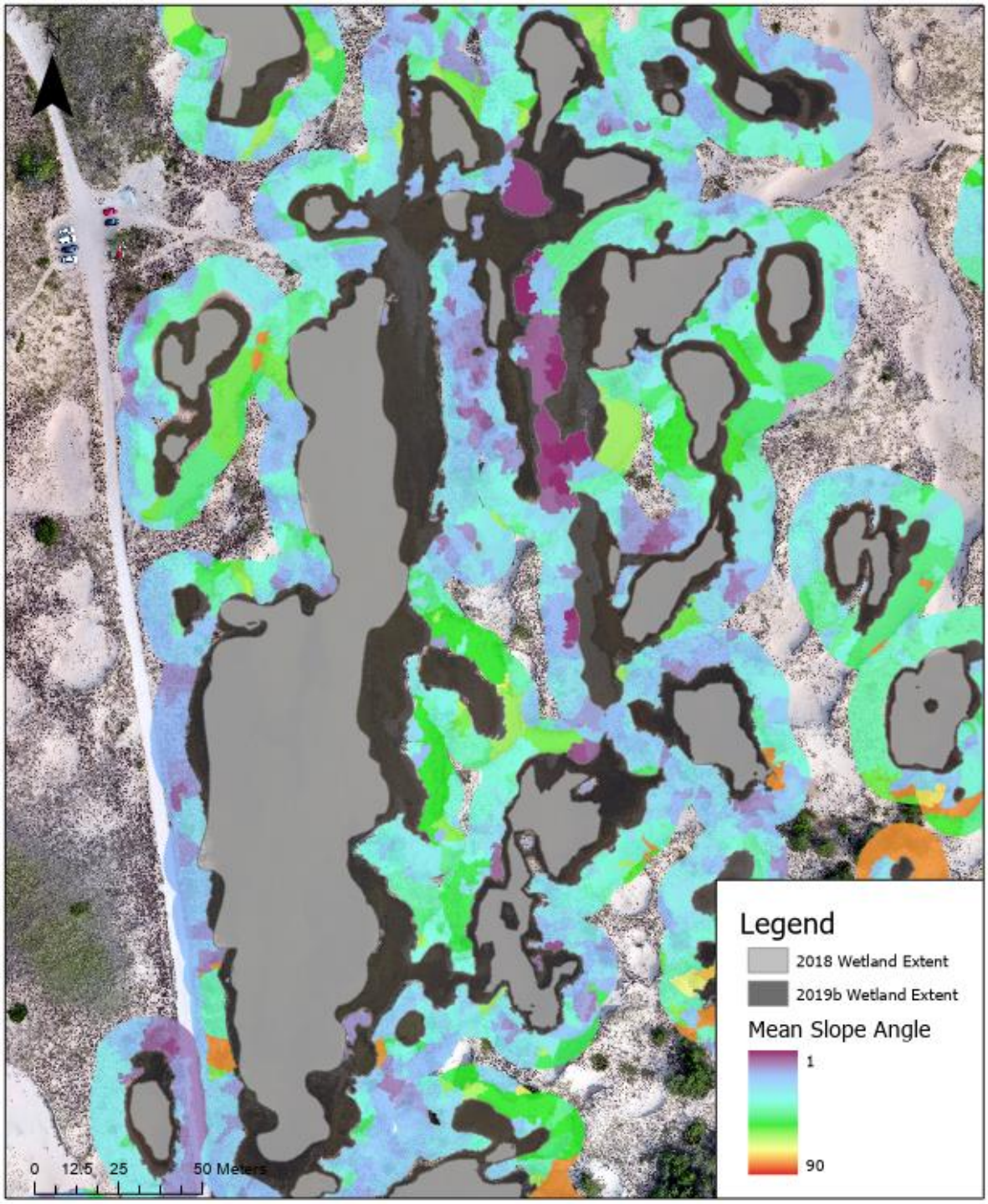

Figure 17. Largest wetland in 2019 with proximal slopes.

Vegetation

In 2018 there was an OBIA limitation in terms of spatial resolution compared to 2019, and small clusters of sparse vegetation were not possible to extract. This study quantified the

annual stability rate of dense vegetation 1.61% increase to 2019a and 1.66% monthly increase to 2019b, expanding from 28,586.46 m^2 in 2018 to 46,113.3 m^2 in 2019a to 47,452.67 m^2 in 2019b. The sparse vegetation almost doubled from September to October with a 1.73% increase, expanding from 86,285.34 m^2 to 149,138.70 m^2. Referring to Figure 17 and 24, the sparse vegetation coverage provides evidence of wetland stabilization.

Table 7. Land Cover Changes at Ludington State Park, 2018-2019. ([2018 to 2019a; 2019a to 2019b])

		Area (m^2)		
	Year	**2018**	**2019a**	**2019b**
Land Cover	**Wetland**	52,521.76	74,577.6 [+1.42%]	82,501.33 [+1.32%; +1.11%]
	Vegetation - Sparse	...	86285.34	149138.70 [+1.73%]
	Vegetation - Dense	28,586.46	46,113.3 [+1.61%]	47,452.67 [+1.66%; + 1.06%]

RESULTS

Statistical Analysis

Correlations with wetland growth

A Spearman's rank-order correlation was used to assess the relationship between wetland growth percentages and aspect, mean slope, and object-based change detection features of vegetation densities. One hundred and forty wetlands were analyzed. Statistically significant positive correlations were observed between annual wetland growth percentage and the dominant slope aspect of each quadrant, monthly sparse vegetation growth, and negative correlations with annual dense vegetation growth, annual dense vegetation loss, monthly dense vegetation growth, monthly dense vegetation loss, and monthly dense vegetation changes, monthly sparse vegetation loss, and percent rise of slope (see Table 8).

Table 8. Correlations of annual wetland growth percentage.

			Annual Wetland Growth Percentage
Spearman's rho	Annual Wetland Growth Percentage	Correlation Coefficient	1.000
		Sig. (2-tailed)	
		N	760
	Aspect	Correlation Coefficient	.077*
		Sig. (2-tailed)	0.034
		N	760
	Slope	Correlation Coefficient	-.150**
		Sig. (2-tailed)	0.000
		N	760

Table 8 - continued

Monthly Dense Growth Percentage	Correlation Coefficient	-.227**
	Sig. (2-tailed)	0.000
	N	760
Monthly Dense Loss Percentage	Correlation Coefficient	-.163**
	Sig. (2-tailed)	0.000
	N	760
Annual Dense Loss Percentage	Correlation Coefficient	-.224**
	Sig. (2-tailed)	0.000
	N	760
Annual Dense Growth Percentage	Correlation Coefficient	-.206**
	Sig. (2-tailed)	0.000
	N	760
Monthly Sparse Loss Percentage	Correlation Coefficient	-.269**
	Sig. (2-tailed)	0.000
	N	760
Monthly Sparse Growth Percentage	Correlation Coefficient	.075*
	Sig. (2-tailed)	0.039
	N	760

The wetland growth's positive relationships, albeit weak relationships, between majority slope aspect and sparse vegetation signifies that the directionally of slopes within the buffers is important factor when analyzing wetland growth and with increased sparse vegetation. These positive correlations indicate that western facing slopes have more wetland growth.

Directional quadrants of wetland buffers

A one-way ANOVA was conducted to determine the difference between wetland buffer cardinal quadrants relating to annual wetland growth percentage. The quadrants were classified into four groups: north (n = 198), east (n = 183), south (n = 189), and west (n = 190). The quadrants numbers are unequal due to outer wetlands extending past the study area. Data is

presented as mean ± standard deviation. The wetland growth percentages increased from the south (14.93 ± 9.85), west (15.78 ± 11.32), east (17.19 ± 11.60), and north (18.61 ± 23.94), in that order; the cardinal direction quadrants significantly affected mean annual wetland growth percentage, $F(3,756) = 3.833$, $p = .010$ (Figure 18). Wetland expansion is highest in the north quadrants with east quadrants closely behind, suggesting that on average, the north and east quadrants are less stable than the south and west quadrants.

Another one-way ANOVA was conducted to determine the difference between the same cardinal quadrants and monthly sparse and dense growth percentages. The sparse growth percentage increased from east (21.39 ± 13.86), north (22.52 ± 14.59), south (23.97 ± 15.43), and west (23.98 ± 14.22), in that order; the directionality of the quadrants significantly affected mean monthly sparse vegetation growth percentage, $F(3,376) = 0.530$, $p = 0.662$ (Figure 19). The dense growth percentage increased from north (2.25 ± 4.39), east (2.56 ± 4.73), south (2.56 ± 5.01), and west (3.09 ± 14.22), in that order; the directionality of the quadrants are significantly related with the mean monthly dense vegetation growth percentage, $F(3,376) = 0.447$, $p = 0.72$ (Figure 20). In summary, dense and sparse vegetation growth is higher in the west and south, while productivity is comparability low in the north and east quadrants and have more wetland expansion.

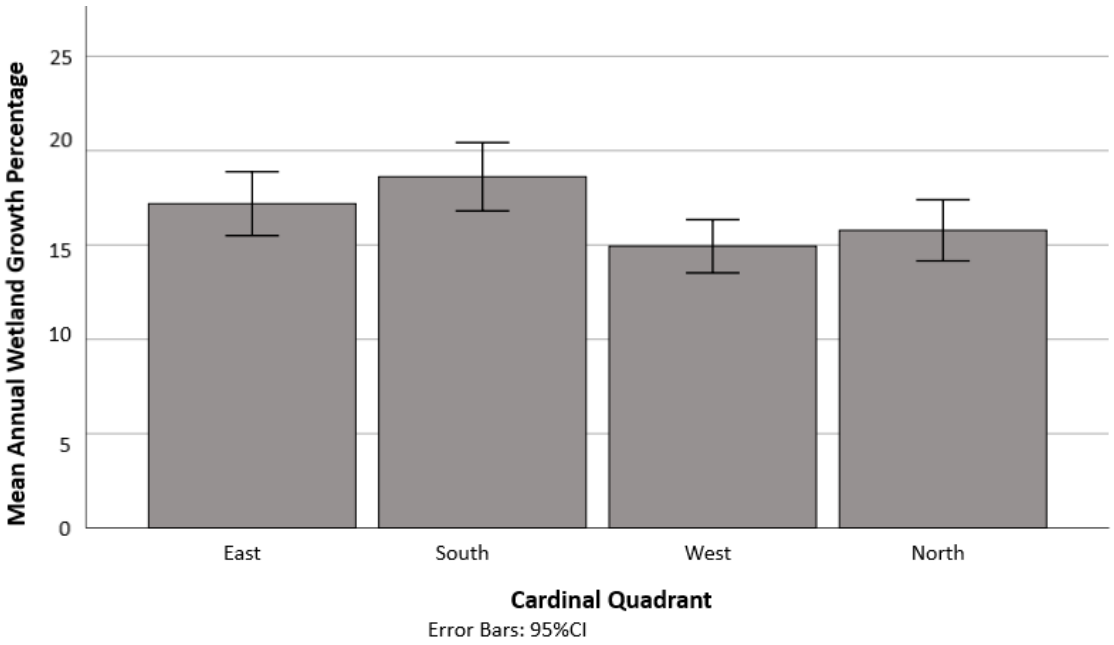

Figure 18. ANOVA mean difference of annual wetland growth percentage by cardinal quadrants.

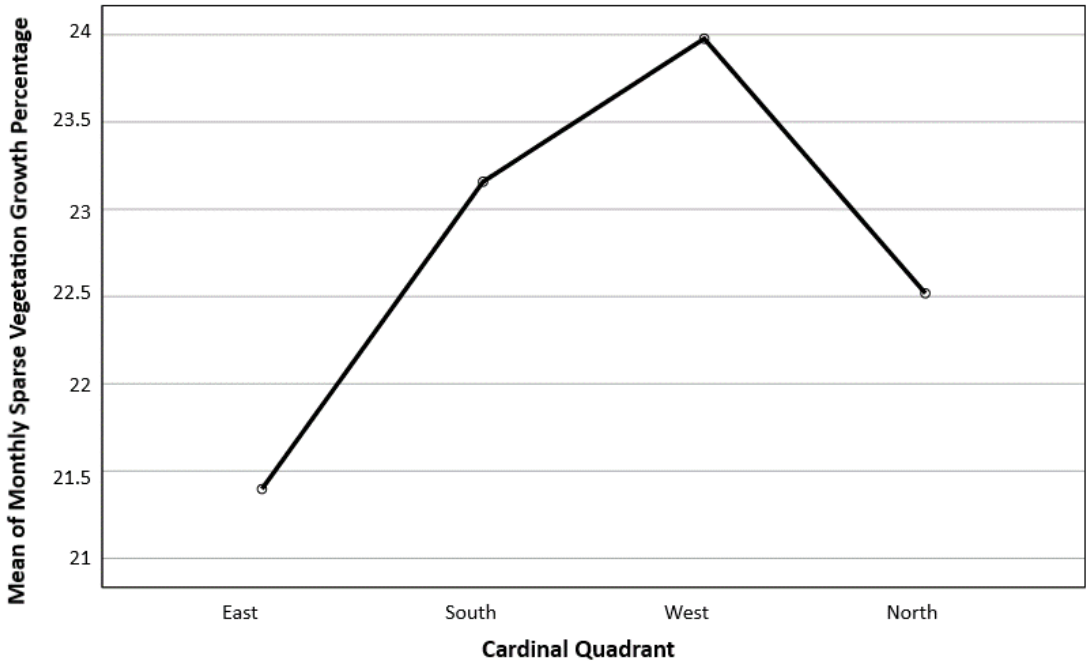

Figure 19. Means plot of cardinal direction quadrants and monthly sparse vegetation growth percentages.

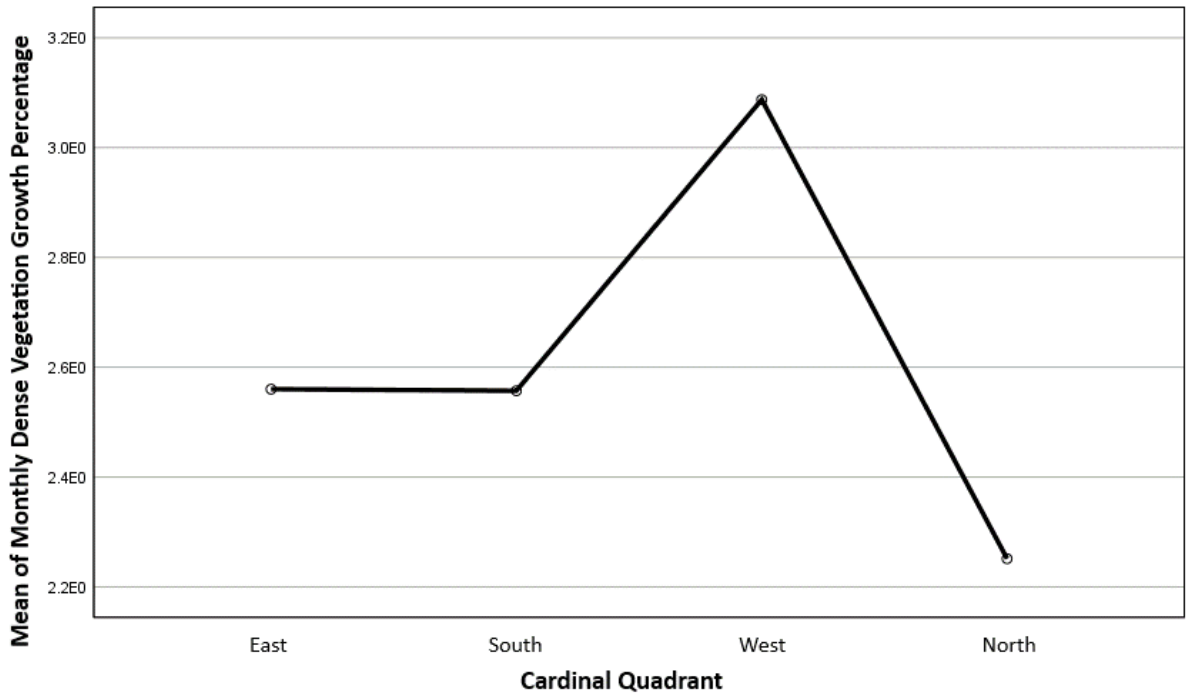

Figure 20. Mean line plot of cardinal direction quadrants and monthly dense vegetation growth percentages.

Factor reduction

A principal component analysis (PCA) was run on several variables of object-based change detection feature coverage in cardinal quadrant buffers, wetland area, predominant aspect, distance to coast, and mean slope. The suitability of PCA was evaluated prior to analysis to confirm that the results were appropriate to run a linear regression. Inspection of the correlation matrix showed that all variables had at least one correlation coefficient greater than 0.3. The overall Kaiser-Meyer-Olkin (KMO) measure was 0.79 with individual KMO measures all greater than 0.7. Bartlett's Test of Sphericity was statistically significant ($p < .0005$), implying that the data was likely factorizable (see table 9).

Table 9. PCA Kaiser-Meyer-Olkin and Bartlett's scores.

Kaiser-Meyer-Olkin Measure of Sampling Adequacy.		
Bartlett's Test of Sphericity		.790
Bartlett's Test of Sphericity	Approx. Chi-Square	3008.383
	df	28

PCA revealed three components that had eigenvalues greater than one and explained 47.4%, 14.76%, 13.4 % of the total variance, respectively. Visual inspection of the scree plot indicated that only the three components should be retained; the third component is the inflation point that represents the point at which the graph beings to level out and the remaining components add little value to the total variance (Figure 21). The three-component solution explained 75.75% of the total variance. A Varimax orthogonal rotation was used to help interpretability. The rotated solution exhibited a complex structure, indicating the same variables are used in each loading and factor analysis, but have different loadings (Table 10).

The main objective for the factor reduction through PCA is to understand the patterns of correlations between the original variables and create linear composites of the original variables for new indicators through shared properties. The score loadings were saved to run a regression model. The first component loading, scored high with distance to shoreline, slope, and annual dense vegetation changes, referred to as latitudinal succession loading. The second component loadings have high loadings of monthly dense growth and monthly sparse loss, referred to as vegetation development. The third component loadings scored high with aspect and monthly sparse growth, referred to as productivity of slope. These factor scores are the linear composite

of the optimally weighted original variables calculated automatically by SPSS statistics; essentially a weighted sum of the variables in each component.

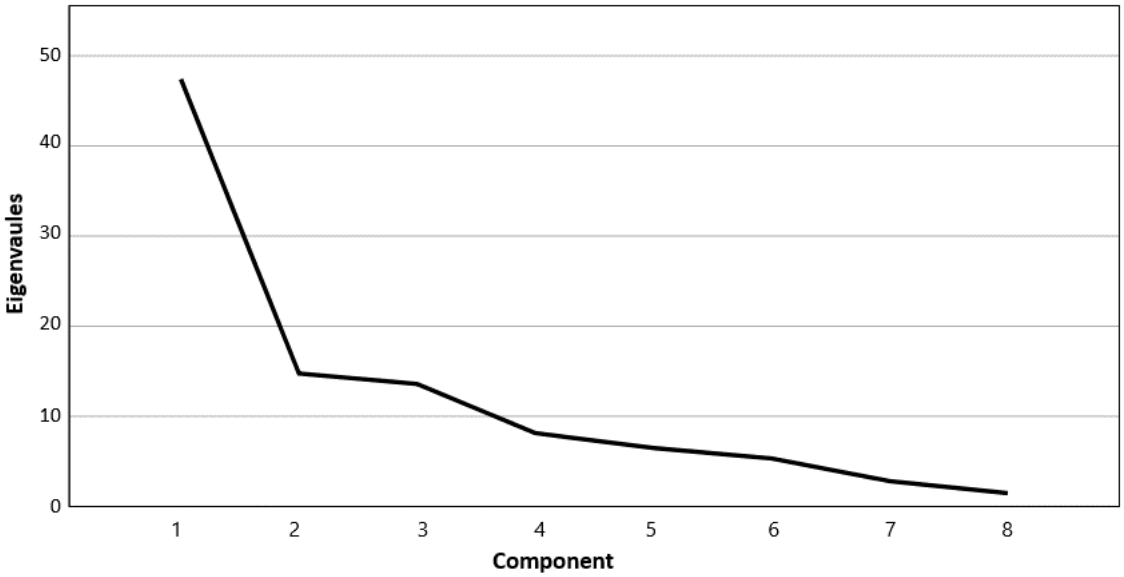

Figure 21. Principal component analysis scree plot.

Table 10. Rotated component matrix[a] of factor reduction.

Variables	Component		
	Succession	Vegetation Development	Productivity of Slope
Distance to Shoreline	.851	-.004	.050
Mean Slope	.896	.251	-.101
Percent Area of Monthly Dense Growth	.369	.725	-.048
Percent Area of Annual Dense Loss	.735	.112	-.159
Percent Area of Annual Dense Growth	.835	.424	-.019
Percent Area of Monthly Sparse Loss	.024	.906	.026
Percent Area of Monthly Sparse Growth	-.434	-.365	.573
Aspect	.047	.105	.923

Extraction Method: Principal Component Analysis.
Rotation Method: Varimax with Kaiser Normalization.[a]
a. Rotation converged in 4 iterations.

Wetland growth regression

A linear regression was run to understand the effect of environmental influences and change detection features on wetland stability. To assess linearity a scatterplot of the three PCA components regression factor scores superimposed a regression line and was plotted along with histogram of the dependent variable. Visual inspection of these two plots indicated a linear relationship between the variables. There was homoscedasticity and normality of the residuals. The regression equations for PCA 1-3 are: wetland growth percentage = 94.67 – 32.37* latitudinal succession , 95% CI [-45.978, -18.755]; wetland growth percentage = 94.67 – 42.07 * vegetation development, 95% CI [-55.686, -28.462]; wetland growth percentage = 94.67 – 157.08 * productivity of slope, 95% CI [-171.692, -144.468]. The three components statistically and significantly predicted wetland growth areas, $F(3, 756) = 192.787$, $p < .0005$, accounting for 43.3% of the variation in wetland growth area with adjusted $R^2 = 43.1\%$ (refer to Tables 11-13 and Figures 22 and 23).

The R^2 value of 43.1% represent the percentage of variance of wetland growth that can be explained by the PCAs. The regression analysis show there is a negative relationship between the dependent variable, Annual Wetland Growth, and the independent variable included in the PCA. The p-value of 0.0005 provides enough evidence to reject the null hypothesis of that annual wetland growth is not influence by any of the independent variables. The coefficients for succession, vegetation development, and productivity of slope are as follows: -32.37, -42.07, and -157.08; from the regression equation, the prediction can be make that if there is an increase of PCA factor scores, annual wetland growth decreases, i.e. wetlands will have more stability.

Table 11. R-square values for regression model.

Model Summary[b]

Model	R	R Square	Adjusted R Square	Std. Error of the Estimate
1	.658[a]	.433	.431	191.028355370928

a. Predictors: (Constant), Regression Factor Score for PCA1, PCA2, and PCA3

b. Dependent Variable: Annual Wetland Growth Area

Table 12. ANOVA of regression model.

ANOVA[a]

Model		Sum of Squares	df	Mean Square	F	Sig.
1	Regression	21105482.661	3	7035160.887	192.787	.000[b]
	Residual	27587825.412	756	36491.833		
	Total	48693308.073	759			

a. Dependent Variable: WGY_AREA

b. Predictors: (Constant), Regression Factor Score for PCA1, PCA2, and PCA3

Table 13. Regression coefficients for PCA components.

		Regression Model			
		(Constant)	Succession	Vegetation Development	Productivity of Slope
Unstandardized Coefficients	B	94.673	-32.366	-42.074	-158.080
	Std. Error	6.929	6.934	6.934	6.934
Standardized Coefficients	Beta		-.128	-.166	-.624
t		13.663	-4.668	-6.068	-22.798
Sig.		.000	.000	.000	.000
95.0% Confidence Interval for B	Lower Bound	81.070	-45.978	-55.686	-171.692
	Upper Bound	108.276	-18.755	-28.462	-144.468
Correlations	Zero-order		-.128	-.166	-.624
	Partial		-.167	-.215	-.638
	Part		-.128	-.166	-.624
Collinearity Statistics	Tolerance		1.000	1.000	1.000
	VIF		1.000	1.000	1.000

a. Dependent Variable: Area of Annual Wetland Growth

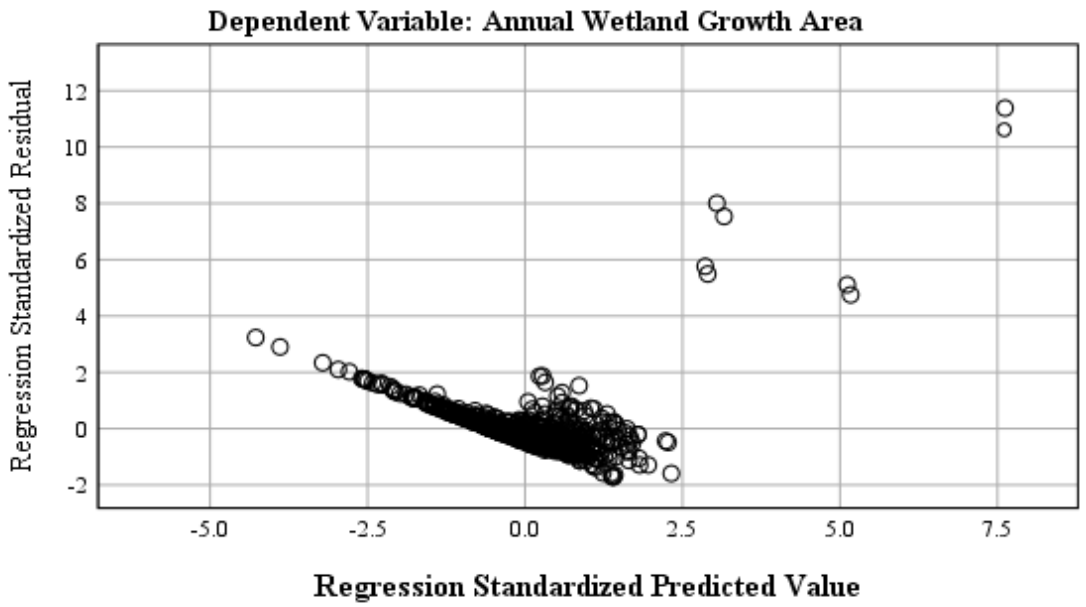

Figure 22. Regression scatterplot of annual wetland growth area.

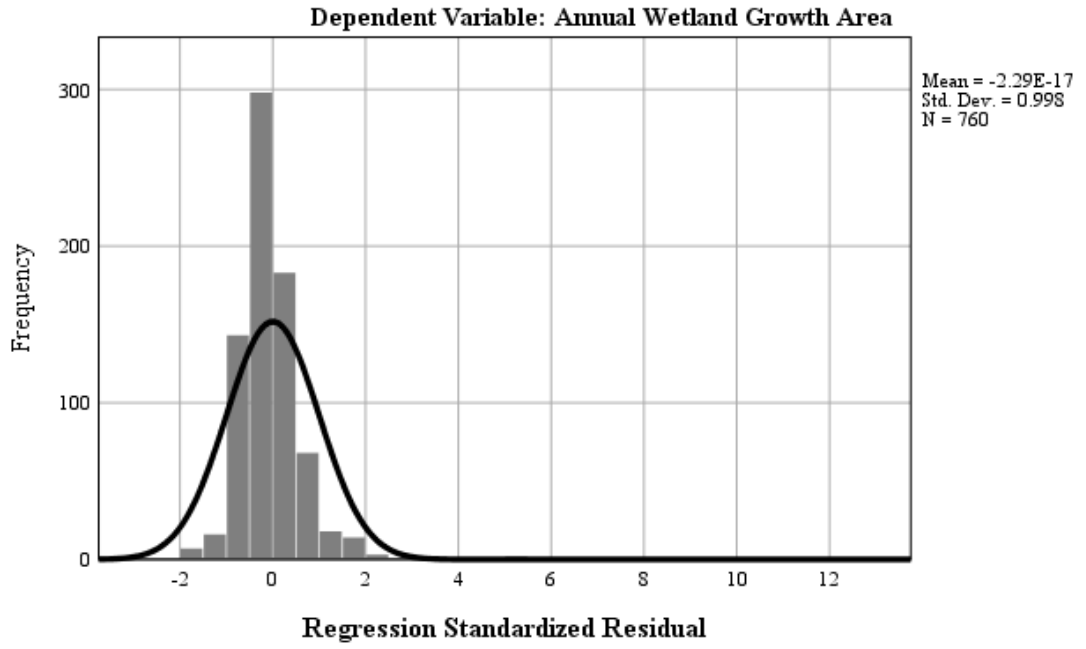

Figure 23. Histogram of annual wetland growth.

Summary

Abiotic factors included in the statistical analysis are distance to the coast, direction of slope, and percent rise of slopes. With the 5 and 10-meter buffers and their divided cardinal quadrants, every wetland was attributed eight different sets of data. However, after testing the

differences of buffer sizes, it has been confirmed that both buffer distances produce the same results in the regression equation. Moreover, the 5-meter buffer can be dropped from the analysis and the results are the same.

Wetland growth is negatively correlated with distance to coast and percent rise of slope, the farther away a wetland is from the shore, the angle of slope increases making wetland growth unfavorable The cardinal direction quadrants of wetland buffers show that annual wetland expansion is more likely to occur in the north and east quadrants with mean wetland percentages over 17 rather than west and south with mean wetland percentages under 16. However, the north and east quadrants have higher standard deviations than west and south. This also provides insight that more vegetation is along the west and south quadrants. The largest wetland (refer to Figure 17) in 2019 experienced the amalgamation of 7 directly proximal wetlands. Additionally, neighboring wetlands experienced a union of 2 or more, which proves the necessity of quantifying surrounding vegetation that contributes to stabilization. This wetland has very low-lying slopes to the northeast, as well as less vegetation clusters. Implying that the lower the slope, the less resistance of wetland expansion, perhaps aid the directional flow.

The slope direction polygons with attributed slope percent provided insight were sparse and dense vegetation are more likely to be found, while significant wetland expansion occurs is area with relatively low slopes. Based on the sun azimuth and radiation, vegetation is more like to grow in the north and east quadrants. However, based on the evidence that sparse vegetation is more prevalent in the west and south quadrants, we can assume that these specific vegetation species pioneer on the windward side of the slope relative to the wetland. In most cases, through fieldwork observation as well, the vegetation structures reduce erosion and even influence sand

buildup, and on the leeward side a there is little vegetation formed, often open sand, to meet the wetlands.

DISCUSSION

Interdunal wetlands provide an especially challenging environment for landscape ecology research due to their extremely dynamic nature. However, Ludington State Park is designated a critical dune area and any research conducted to understand the ecosystem is noteworthy. This research on interdunal wetland landscape ecology relied heavily on geospatial tools and techniques and answered research questions regarding the spatial distribution of environmental influences and change rates.

UAS and GIS Applications in Interdunal Wetland Research

This study involved various applications to answer the proposed questions. Commonly in exploratory applications research, adaptions are necessary to reduce the amount of limitations and uncertainties. Unfortunately, UAS flights were not permitted for most of the growing season and reduced fieldwork dates from the proposed five to two, limiting research at the end of the growing season. Additionally, without high temporal datasets, it was not possible to accurately classify specific vegetation species based on phenology and spectral signatures (Yan et al.,2018) UAS flights covered a total area of 0.369 km^2 at 390 ft (119 m) above the surface with a high spatial resolution of 3 cm.

Keypoint matching across images for both 2019a and 2019b passed the quality check in Pix4D. An average of 97.5% of images were calibrated with a mean of 30,972 matches per image for 2019a and 23,568 matches for 2019b during SfM processing. The amount of keypoints and matches are typical for SfM. One of reasons that may explain the lower match amount in

2019b was an offset in camera calibrations that created too much exposure in images to detect enough keypoints. From GCPs, an absolute reference system was used for georeferencing, a crucial element for orthomosiacs and ultimately, accurate delineation of features and their size, shape, and orientation. The DSMs created from SfM-MVS added value to both OBIA classification and spatial analysis (Mathews, 2015). With visual interpretation of the DSMs alone, it was possible to predict the landscape features, specifically wetland areas and dense vegetation, based on the terrain attributes (Bou Keir et al, 2010).

OBIA classification results extracted meaningful vegetation densities of growth and loss and wetland growth and loss features for spatial analysis by applying specific parameters, in this case 18.5 spectral, 17 spatial, and a minimum segment size of 50 pixels (Ellis and Mathews, 2018). The high resolution of imagery allowed the supervised classification to delineate clusters of sparse vegetation in 2019. By compositing the imagery with DSMs, dense vegetation was easily extracted. One of the challenges of OBIA in wetland ecosystem previously mentioned is the moisture content of the sand, especially areas within a meter of the wetland (Delgado-Fernandez et al., 2009). The OBIA frequently classified these areas as water, or even sparse vegetation, due to the naturally shallow edges of the wetland, saturated nearby sand, and limited senor capabilities. Most research involving OBIA application has an overall accuracy score near or about 90% (refer to Table 2), this study's maximum overall accuracy was 67%, supporting the decision to edit 2018, 2019a and 2019b's classification results through manual digitization.

This study explored numerous analysis tools and many adaptations were made to understand the spatial patterns and tendencies of interdunal wetlands. To evaluate change detection, the assessment involved comparing the size and shape of features from different dates and calculating portion of one date features within a feature from another data (Lightfoot et

al.,2020). A deeper understanding of the relationship between vegetation and wetland stabilization was achieved by calculating the geometry attributes of area and percentage, rather than attributing wetland buffer areas with presence and no presence. Aspect polygons provided insight and confirms that sun insolation is important to understand where sparse and dense vegetation is more likely to grow.

Statistical Analysis Results

Cardinal quadrant of natural processes

The cardinal direction quadrants added considerable value to analysis, not only to examine the average slope direction, but to analyze which portions of the wetland are more susceptible to environmental influences rather than the entire wetland. The south quadrant has the lowest mean percentage of wetland growth, there are several factors that could influence this including less wind disturbance from higher slopes, less vegetation productivity, and distance to the shore. The west and east quadrant have similar means, but the assumption can and should be made that the west quadrant has more stabilizing factors compared to the east quadrant.

There is higher coverage of sparse vegetation in the west and south quadrants of the wetlands compared to the north and east quadrants. The slopes of south and west quadrants are primarily facing to the north and east, where the more predominant sun influencing increased productivity of vegetation. The significant increase of vegetation corresponds to the natural processes of open and close dune complexes. The grass and shrubs considered as sparse vegetation is adapted to withstand constant sand burial and strong winds, while sparse vegetation is consistently buried, the roots continue to stabilize the soil and accumulate organic soil for further primary vegetation growth that progress into secondary and tertiary growth.

Both monthly sparse and dense vegetation growth is highest in the west and south quadrants, respectively. Thus, the north and east quadrant areas are less fitting for vegetation growth due to high sun insolation and temperatures. By comparing the difference of means of monthly vegetation growth, a predication was made that north and east quadrants with the lowest vegetation growth means, have the highest wetland growth means. The first ANOVA comparing wetland growth confirms the relationship that quadrants with low vegetation growth has a negative relationship with wetland growth.

Factor reduction

The eigenvalues in PCA greater than 1 are considered significant and implies that loading patterns are meaningful. while the varimax factor score in the rotate component matrix great than 0.6 is considered as a strong value range in loadings. The three component loadings partitioned the original variables in a meaningful way to interpret various elements of the ecosystem: latitudinal succession, vegetation development, and productivity of slopes. The latitudinal succession explains dense vegetation is more prevalent in the backdune, where there in more stable ground for dune to grow. The vegetation development explains the natural process of primary, secondary, and tertiary vegetation growth, while the productivity of slope explains how biogeographical distributions of the environment play an important role in vegetations productivity.

Regression

The regression coefficients for PCA succession, vegetation development, and productivity of slope represent the mean change of wetland growth. For every additional factor score in succession, vegetation development, and productivity of slope the wetland growth will decrease. The succession PCA loading was high in distance to shoreline, slope, and annual dense

vegetation changes suggesting there is a latitudinal gradient of dune succession extending inland. The vegetation development PCA loading was high in monthly dense growth and monthly sparse loss confirming that primary growth, sparse vegetation will eventually be replaced by secondary growth, dense vegetation. The productivity of slopes PCA loading scored high in aspect and monthly sparse growth indicating that directionality of sun insolation and wind prevalence is an important consideration when monitoring primary vegetation growth.

Spatial Distributions of Natural Processes and Interdunal Wetland Stability

LSP has distinctive interdunal zones; beach, foredune, interdunal wetland, and backdune which progress latitudinally with mixed blowouts and dune fields. Then natural processes of sand conveyance by waves and current occur at the beach and extending to the foredune, then wind carries sand farther inland to building the backdune. However, the human use of the beach, particularly the dirt/sand road stretching north-to-south through the study area, directly effects the ecosystem's dynamics. This road is located in the trough of the foredune and backdune, and it is evident that it restricts the adjacent backdune growth, continuing the expansion of the foredune and interdunal wetland.

Wetland stabilization relies heavily on surrounding vegetation and the accumulation of organic soil, dune slopes and vulnerability of erosion, and distance to the coast. The annual and monthly dynamics of wetlands and vegetation were quantified. Monthly mean water-levels of Lake Michigan corresponding to data acquisition dates are as follows: July 2018 - 566.92ft, September 2019 - 5881.63 ft, and October 2019 - 581.66 ft (US Army Corps of Engineers, 2019). The wetlands and Lake Michigan water-levels are in synchrony; the 21.71 ft increase from 2018 to 2019a supports the annual change rate of wetlands of +1.42% increase and the small increase from 2019a to 2019b accounts for the monthly increase of 1.11%.

The distinct water movements, inflow and outflow, and variation of organic soil affect wetland size (Brinson, 1993). The largest wetland, refer to Figure 17, is an example of drastic water movement, and thus, influenced multiple wetland amalgamation. After visual interpretation of each DSM, the slopes around the wetland continued to decrease. This wetland is also adjacent to dirt road that has, without a doubt, influenced the dynamics of vegetation, dune, and wetland growth. Additionally, neighboring wetlands experienced a union of 2 or more, which proves the necessity of quantifying surrounding vegetation that contributes to stabilization. Figure 18 shows sparse vegetation surrounding the largest wetland; no dense vegetation is present around this wetland. The northeast portion has large areas of open sand with relatively low slopes, this provides insight on the importance of sparse vegetation presence.

When wetlands are surrounded by majority dense vegetation, there is less change because of higher accumulation of organic soil and less susceptibility of wind and water erosion. Additionally, distance from the shoreline and mean percent rise of slope coincide with annual dense vegetation change. The increased slopes indicate natural succession stages, where the sand becomes more stable as vegetation continues into secondary and tertiary growth, catching mobile sand, growth in dune structure, and accumulating more organic matter. The positive relationship of this these factors signifies that there is west to east gradient of presence of dense vegetation developing farther away from the shoreline. Furthermore, wetlands situated at the bottom of steep slopes with dense vegetation are less likely to expand and the more gradually the slope is the more wetland growth with take place

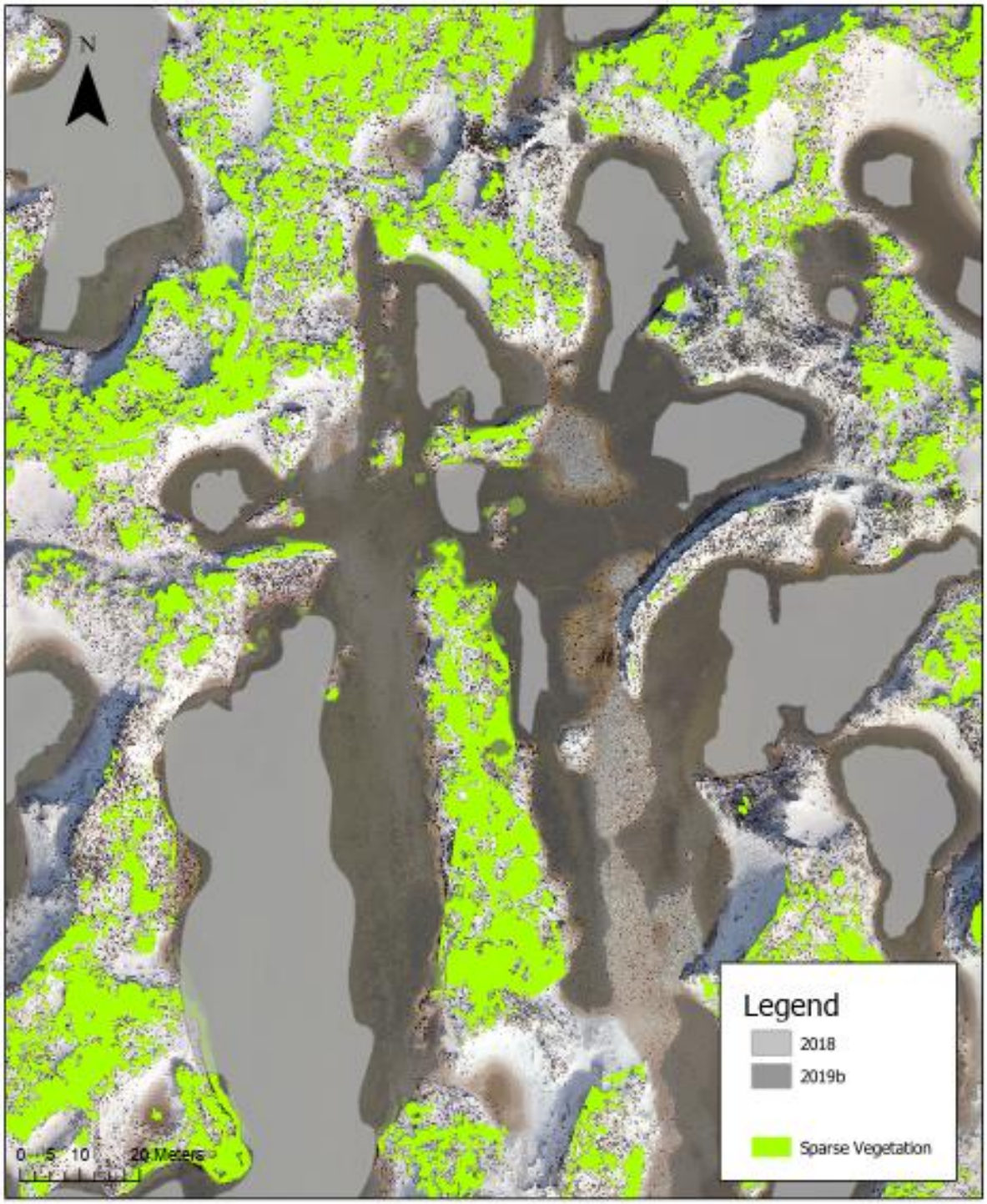

Figure 24. Northern portion of the largest wetland in 2019 with surrounding sparse vegetation.

Plant communities dependent on spatiotemporal patterns in water availability. Natural processes of dune growth and regression develop over several types of land cover within a wetland, providing a unique niche for flora and fauna. The produced comparisons of 2018,

2019a, and 2019b wetlands and densities of vegetation, with attributed change proportions of the total area and percentage gave insight to the nature, significance, and spatial distribution and patterns of interdunal wetland ecosystems (Lightfoot et al., 2020). While extracting vegetation and wetland features through OBIA, is was apparent that vegetation structures fluctuate throughout the dune system and confirms there is a latitudinal, succession gradient from west to east. After extracting vegetation features from 2018, 2019a, and 2019b, environmental influences such as prevailing winds, sand mobility, high insolation, beach use have substantial effects on early successional plant communities.

The foredune zone is where the pioneer (sparse) vegetation is established. There is a correlation between distance to the shore and sparse vegetation growth. The backdune zone of LSP is where the majority of dense vegetation is found. There is a negative correlation between sparse and dense vegetation, meaning if there is more sparse growth it does not necessarily mean there is dense vegetation loss; rather, the dense vegetation needs pioneer species, sparse vegetation, to establish growth in. The sparse vegetation is adapted to withstand strong prevailing winds, high insulation, and fluctuations in water availability. Dense vegetation can only grow after sparse, and commonly take the place of sparse, meaning as sparse vegetation loss percentages go down dense growth percentages go up with increasing distance from the shoreline.

In the northern hemisphere, an inference can be made that south facing slopes receive more sunlight, and thus, grow more vegetation. However, vegetation growth is more predominant in west and south quadrants. While the cardinal quadrants represent the generalization of slope direction directly at the wetland edge, the buffer extends 10 meters and captures the opposite slope leading up the dune peak which quickly reaches the wetland edge. To

further explain, the majority of vegetation growth summarized within the buffers is on the windward side relative to the center of the wetland. Furthermore, the west and south facing slopes leading up to the peak are found in the west and south quadrants that have more vegetation growth. The north and east quadrants have low vegetation growth which make it easier for wetlands to expand further out in those quadrants, even more so in areas with low lying slopes.

Additionally, over time in these dune systems, blowouts occur where sparse vegetation stabilization does not provide enough resiliency to wind erosion. When blowouts occur (see Figure 25), the depression continues to deepen, often steep slopes, by wind and creates an area for interdunal wetlands to form. This natural process in particular is important in research monitoring wetlands because of blowouts proximity to the coast and the susceptibility to abiotic factors. If a blowout occurs closer to the beach, one can expect extreme changes due to sand erosion and waves that could influence the blowout expanding inland. If the blowout is located in the backdune, it can be expected that dense vegetation continues to stabilize the ground and even build up the dune by catching sand from wind transportation.

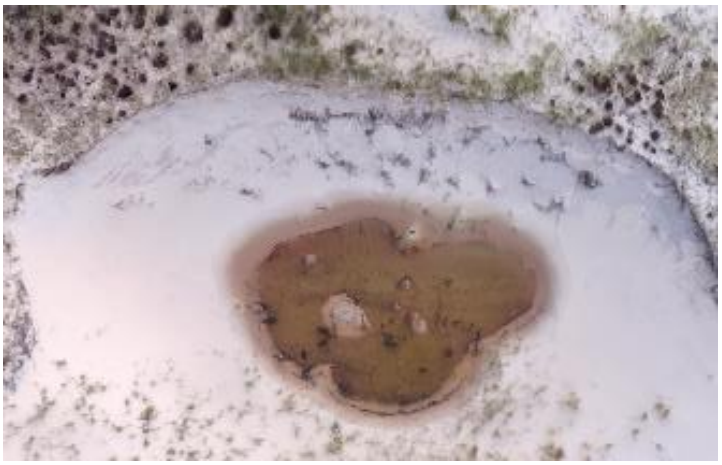

Figure 25. Example of a blowout forming a pocket for wetland development due to vegetation erosion.

Limitations

Data acquisition

Timing of imagery should be improved, over a year between observations and over a single month, so not constant with timing. For comprehensive annual and monthly change rate, it is better to have multiple time intervals observed and determine the average change of all intervals. Additionally, spatial resolution restriction has significantly limited that amount of analysis that can be conducted. The assumption that small and shallow wetlands in 2018, as well as sparse vegetation structures were not extracted from OBIA and the wetland change rate could be drastically less.

Modifiable Areal Unit Problem (MAUP)

MAUP affected results when point-based measures of spatial phenomena are aggregated into wetland buffers. There was statistical bias that has impacted the results of statistical research tests, specifically the cardinal quadrants and direction of slope. For instance, the created slope aspect polygons were summarized to get the mean direction of slope within the buffer; some buffers contained over 15 separated direction features. Therefore, the connection between mean direction of slope depends on the size of buffers and slope aspect polygons for which data are reported. The aggregation of the smaller aspect features renders heightened bias and correlation areal size of buffers increases. Furthermore, the aggregation of direction of slope discards the variation in correlation statistics caused by the regrouping of aspect into different configurations at the same scale of the buffers.

Future Research

Recommendations for future research in monitoring the change of interdunal wetlands should include improved data acquisition and sensor abilities, inclusion of wind and precipitation

patterns, heavier use of DSMs, methodology for cardinal direction quadrants, less data aggregation, and potentially interpolation methods for environmental constraints. Improved data acquisition includes higher frequency of UAS flights over several years in the growing season to approximate consistent annual and monthly change rates. If hyperspectral sensors are used for extraction of emergent and benthic vegetation the understanding the overall productivity taken place within wetlands is improved. Wind patterns and strength of wind gusts could be used to interpolate surface vulnerability of erosion. Precipitation patterns provide insight changed rates of wetland expansion and loss. In this study, DSMs were only used to aid OBIA and calculate slopes, but DSMs have the potential to interpolate the depth of wetlands or path distances rather than Euclidean distance. The cardinal quadrant may have had better results if the Euclidean direction tool used with the wetland centroids and reclassifying for only the 4 major direction rather than using the subdivide tool with equal area. Less data aggregation decrease the effect of MAUP; however, machine learning and automation may be necessary to handle to the large datasets.

CONCLUSION

This research on interdunal wetlands sought to advance our understanding of ecosystem dynamics and associated environmental influences. The results of the research show that UAS remote sensing and geospatial analyses is necessary to interpret, monitor, and analyze the a highly dynamic ecosystem. The main finding of this study is where there is more productivity of vegetation, the more stable the soil and sand is aiding constant wetland levels. Additionally, vegetation structures within dune complexes are conditioned to withstand the strong prevailing southwest winds. The west and south cardinal quadrants experience more wetland stability. The west and south quadrants are areas where more vegetation growth is found, providing sand stability and wind divergence. The north and east quadrants are areas where wetland expansion is likely to occur due to low vegetation presence.

Vegetation and slopes increase as distance to the shoreline increase, especially in the backdune zone, because there is less wind erosion allowing dense vegetation to establish, and thus, catching wind transported sand to build up the dune. The negative correlations with dense vegetation change indicate that wetland growth is unlikely when there is presence of dense vegetation. The slope has a negative relationship with wetland growth as well, implying that wetlands situated at the bottom of steep slopes are less likely to expand and the more gradually the slope is the more wetland growth with take place. LSP exhibits a interdunal wetland latitudinal succession gradient.

As for ongoing biodiversity study of Lake Michigan's interdunal wetlands, this research provides insight on the importance of the biogeographical distribution of vegetation. Vegetation has the upmost importance of wetland stability, which affects macroinvertebrate community structures, spatial and temporal pattern of amphibians, food-chains, and landscape-level genetic pattern. For future diversity sampling, fieldwork should focus on the southwest portion of wetlands. With higher presence of vegetation in these portions provide a niche habit for species of the study's interest.

APPENDIX. **List of object-based image analysis feature classes included in statistical analysis.**

OBIA Delineation		
NLCD Classification	*Thesis Representation*	*Year*
Water	Wetland	2018-2019b
Herbaceous	Sparse Vegetation	2019a-2019b
Mixed Forest	Dense Vegetation	2018-2019b
Barren	Sand	dropped
Object-based Change Detection via Overlay Tools		
WGM	Monthly Wetland Growth	
WGY	Annual Wetland Growth	
SGM	Monthly Sparse Vegetation Growth	
DGM	Monthly Dense Vegetation Growth	
DGY	Annual Dense Vegetation Growth	
Buffer coverage of Object-based Change Detection		
WGM_Percentage	Percentage of Monthly Wetland Growth in Buffer	
WGM_Area	Area of Monthly Wetland Growth in Buffer	
WGY_Percentage	Percentage of Annual Wetland Growth in Buffer	
WGY_Area	Area of Annual Wetland Growth in Cardinal Buffer	
SGM_Percentage	Percentage of Monthly Sparse Vegetation Growth in Buffer	
SGM_Area	Area of Monthly Sparse Vegetation Growth in Buffer	
DGM_Percentage	Percentage of Monthly Dense Vegetation Growth in Buffer	
DGM_Area	Area of Monthly Dense Vegetation Growth in Buffer	
DGY_Percentage	Percentage of Annual Dense Vegetation Growth in Buffer	

REFERENCES

Aber, J. S., Marzolff, I., & Ries, J. B. (2010). SFAP Survey Planning and Implementation. Small-Format Aerial Photography, 119–137. https://doi.org/10.1016/B978-0-444-53260-2.10009-2

Albert, D. (2003). *Between Land and Lake: Michigan's Great Lakes Coastal Wetlands*. Michigan State University and Michigan Natural Features Inventory.

Albert, D. A., Wilcox, D. A., Ingram, J. W., & Thompson, T. A. (2005). Hydrogeomorphic Classification for Great Lakes Coastal Wetlands. *Journal of Great Lakes Research*, *31*(SUPPL. 1), 129–146. http://doi.org/10.1016/S0380-1330(05)70294-X

Arbogast, A. F., Shortridge, A. M., & Bigsby, M. E. (2009). Volumetric Estimates of Coastal Sand Dunes in Lower Michigan: Explaining The Geography of Dune Fields. *Physical Geography*, *30*(6), 479–500. http://doi.org/10.2747/0272-3646.30.6.479

Blaschke, T. (2010). ISPRS Journal of Photogrammetry and Remote Sensing Object-based image analysis for remote sensing. *Journal of Photogrammetry and Remote Sensing*, *65*, 2–16. http://doi.org/10.1016/j.isprsjprs.2009.06.004

Bou Kheir, R., Bøcher, P. K., Greve, M. B., & Greve, M. H. (2010). The application of GIS-based decision-tree models for generating the spatial distribution of hydromorphic organic landscapes concerning digital terrain data. *Hydrology and Earth System Sciences Discussions*, *7*(1), 389–416. http://doi.org/10.5194/hessd-7-389-2010

Brinson, M. M. (1993). Changes in the functioning of wetlands along environmental gradients. *Wetlands*, *13*(2), 65–74. http://doi.org/10.1007/BF03160866

Carrivick, J., Smith, M., & Quincy, D. (2016). *Structure from Motion in the Geosciences.* (First, Vol. 91). Wiley/Blackwell.

Chasmer, L., Hopkinson, C., Veness, T., Quinton, W., & Baltzer, J. (2014). A decision-tree classification for low-lying complex land cover types within the zone of discontinuous permafrost. *Remote Sensing of Environment*, *143*, 73–84. http://doi.org/10.1016/J.RSE.2013.12.016

Chasmer, L., Hopkinson, C., Montgomery, J., & Petrone, R. (2016). A Physically Based Terrain Morphology and Vegetation Structural Classification for Wetlands of the Boreal Plains. *Canadian Journal of Remote Sensing*, *42*(5), 521–540. http://doi.org/10.1080/07038992.2016.1196583

Clarke, S. J., Lamont, K. J., Pan, H. Y., Barry, L. A., Hall, A., & Rogiers, S. Y. (2015). Spring root-zone temperature regulates root growth, nutrient uptake and shoot growth dynamics in grapevines. *Australian Journal of Grape and Wine Research*, *21*(3), 479–489. http://doi.org/10.1111/ajgw.12160

Cohen, J.G., M.A. Kost, B.S. Slaughter, D.A. Albert, J.M. Lincoln, A.P. Kortenhoven, C.M. Wilton, H.D. Enander, and K.M. Korroch. 2020. Michigan Natural Community Classification.Michigan Natural Features Inventory, Michigan State University Extension, Lansing, Michigan.

Corbane, C., Lang, S., Pipkins, K., Alleaume, S., Deshayes, M., García Millán, V. E., … Michael, F. (2015). Remote sensing for mapping natural habitats and their conservation status - New opportunities and challenges. *International Journal of Applied Earth Observation and Geoinformation*, 37, 7–16. https://doi.org/10.1016/j.jag.2014.11.005

Delgado-Fernandez, I., Davidson-Arnott, R., & Ollerhead, J. (2009). Application of a Remote Sensing Technique to the Study of Coastal Dunes. *Journal of Coastal Research*, *255*(5), 1160–1167. http://doi.org/10.2112/09-1182.1

Dronova, I., Gong, P., Clinton, N. E., Wang, L., Fu, W., Qi, S., & Liu, Y. (2012). Landscape analysis of wetland plant functional types: The effects of image segmentation scale, vegetation classes and classification methods. *Remote Sensing of Environment*, *127*, 357–369. http://doi.org/10.1016/j.rse.2012.09.018

Dronova, I., Beissinger, S. R., Burnham, J. W., & Gong, P. (2016). Landscape-level associations of wintering waterbird diversity and abundance from remotely sensed wetland. *Remote Sensing*, 8(6) 462 https://doi.org/10.3390/rs8060462

Dvorett, D., Davis, C., & Papeş, M. (2016). Mapping and Hydrologic Attribution of Temporary Wetlands Using Recurrent Landsat Imagery. *Wetlands*, 36, 431–443. https://doi.org/10.1007/s13157-016-0752-9

Ellis, E. A., & Mathews, A. J. (2018). Object-based delineation of urban tree canopy: assessing change in Oklahoma City, 2006–2013. *Computers, Environment, and Urban Systems*, (August), 0–1. http://doi.org/10.1016/j.compenvurbsys.2018.08.006

EPA. Wetlands Fact Sheet. (2004). Section 404 of the Clean Water Act: How Wetlands are Defined and Identified. Retrieved from https://permanent.access.gpo.gov/websites/epagov/www.epa.gov/OWOW/wetlands/facts/fact11.html

Federal Geographic Data Committee. 2013. Classification of wetlands and deepwater habitats of the United States. FGDC-STD-004-2013. Second Edition. Wetlands Subcommittee, Federal Geographic Data Committee and U.S. Fish and Wildlife Service, Washington, DC.

Frazier, C. (2017) Open interdunal wetland pond. Ludington State Park. photograph

Gallant, A., Gallant, & L., A. (2015). The Challenges of Remote Monitoring of Wetlands. *Remote Sensing*, *7*(8), 10938–10950. http://doi.org/10.3390/rs70810938

Hardin, P. J., & Jensen, R. (2011). Small-Scale Unmanned Aerial Vehicles in Environmental Remote Sensing: Challenges and Opportunities, *GIScience & Remotes Sensing*, 48:1, 99-111. http://dx.doi.org/10.2747/1548-1603.48.1.99

Hardin, P. J., Lulla, V., Jensen, R. R., & Jensen, J. R. (2018). Small Unmanned Aerial Systems (sUAS) for environmental remote sensing: challenges and opportunities revisited. *GIScience and Remote Sensing*, 56(2), 309–322. https://doi.org/10.1080/15481603.2018.1510088

Im, J., Jensen, J. R., & Hodgson, M. E. (2008). Object-Based Land Cover Classification Using High-Posting-Density LiDAR Data. *GIScience & Remote Sensing*, *45*(2), 209–228. http://doi.org/10.2747/1548-1603.45.2.209

Jensen, J. R. (2005). *Introductory Digital Image Processing: A Remote Sensing Perspective*. (D. Kaveney, Ed.) (Third). Pearson Education Inc.

Klemas, V. (n.d.). Remote Sensing of Wetlands: Case Studies Comparing Practical Techniques. *Journal of Coastal Research*, 27(3) 418-427 http://doi.org/10.2112/JCOASTRES-D-10-00174.1

Klemas, V. (2011). Remote sensing techniques for studying coastal ecosystems: an overview. *Journal of Coastal Research*, *27*(1), 2–17. http://doi.org/10.2112/JCOASTRES-D-10-00103.1

Knight, J. F., Tolcser, B. P., Corcoran, J. M., & Rampi, L. P. (2013). The Effects of Data Selection and Thematic Detail on the Accuracy of High Spatial Resolution Wetland Classifications. *Photogrammetric Engineering & Remote Sensing*, *79*(7), 613–623.

Kost, M.A., D.A. Albert, J.G. Cohen, B.S. Slaughter, R.K. Schillo, C.R. Weber, and K.A. Chapman. 2007. Natural Communities of Michigan: Classification and Description. Michigan Natural Features Inventory, Report No. 2007-21, Lansing, MI

LePage, B. A. (2011). Wetlands: A Multidisciplinary Perspective. In Wetlands (pp. 3–25). Dordrecht: Springer Netherlands. https://doi.org/10.1007/978-94-007-0551-7_1

Lichter, 1998 Primary succession and forest development on coastal Lake Michigan sand dunes. *Ecological Monographs* 68:487-510

Lightfoot, P., Scott, C., & Fitzsimmons, C. (2020). Using object-based image analysis with multi-temporal aerial imagery and LiDAR to detect change in temperate intertidal habitats. *Aquatic Conservation: Marine and Freshwater Ecosystems*, *30*(3), 514-531.

Johnson, E. A., & Miyanishi, K. (2008). Testing the assumptions of chronosequences in succession. *Ecology Letters*, *11*(5), 419–431. https://doi.org/10.1111/j.1461-0248.2008.01173.x

Mathews, A. J., & Frazier, A. E. (2017). Unmanned Aerial Systems (UAS). *The Geographic Information Science Body of Knowledge*.https://doi.org/10.22224/gistbok/2017.2.4

Mathews, A. J., (2015).A Practical UAV Remote Sensing Methodology to Generate Multispectral Orthophotos of Vineyards: Estimation of Spectral Reflectance Using Compact Digital Cameras. *International Journal of Applied Geospatial Research, 6(4), 65-87*

Millington, A., Blumler, M., & Schickhoff, U. (Eds.). (2011). The biogeographical distributions: the role of past environments, physical factors, and biotic interactions. *The SAGE handbook of biogeography*. Sage.

Moor, H., Rydin, H., Hylander, K., Nilsson, M. B., Lindborg, R., & Norberg, J. (2017). Towards a trait-based ecology of wetland vegetation. *Journal of Ecology*, *105*(6), 1623–1635. http://doi.org/10.1111/1365-2745.12734

Mui, A., He, Y., & Weng, Q. (2015). An object-based approach to delineate wetlands across landscapes of varied disturbance with high spatial resolution satellite imagery. *ISPRS Journal of Photogrammetry and Remote Sensing*, *109*, 30–46. https://doi.org/10.1016/j.isprsjprs.2015.08.005

Rapinel, S., Clément, B., Dufour, S., & Hubert-Moy, L. (2017). Fine-Scale Monitoring of Long-term Wetland Loss Using LiDAR Data and Historical Aerial Photographs: the Example of the Couesnon Floodplain, France. *Wetlands*, 38, 423–435. https://doi.org/10.1007/s13157-017-0985-2

Rapinel, S., Hubert-Moya, L., & Clémentb', B. (2015). Combined use of lidar data and multispectral earth observation imagery for wetland habitat mapping. *International Journal of Applied Earth Observation and Geoinformation*, *37*, 56–64. https://doi.org/10.1016/j.jag.2014.09.002

Rouse Jr, J. W., Haas, R. H., Schell, J. A., & Deering, D. W. (1973). Monitoring the vernal advancement and retrogradation (green wave effect) of natural vegetation. Silva, T. S. F., Maycira, ·, Costa, P. F., Melack, J. M., Evlyn, ·, Novo, M. L. M., … Novo, E. M. L. M. (2008). Remote sensing of aquatic vegetation: theory and applications. *Environmental Monitoring Assessment*, *140*, 131–145. http://doi.org/10.1007/s10661-007-9855-3

Snavely, N., Seitz, S. M., & Szeliski, R. (2008). Modeling the world from Internet photo collections. *International Journal of Computer Vision*, *80*(2), 189–210. https://doi.org/10.1007/s11263-007-0107-3

Straford and Rooney. (2017) Special Issue – Coastal dune slack hydro-ecology. *Journal of Coastal Conseration* 21(5), 10.1007/s11852-017-0559-8

United States Department of Agriculture - Forest Service. (2006, September 11). *Nordhouse Dunes Research Natural Area - Northern Research Station - USDA Forest Service.* Natural Research Areas. https://www.nrs.fs.fed.us/rna/mi/huron-manistee/nordhouse-dunes/

United States Army Corps of Engineers. (2020, May) Great Lakes Hydraulics and Hydrology – Great Lake Water Level Data https://www.lre.usace.army.mil/Missions/Great-Lakes-Information/Great-Lakes-Information-2/Water-Level-Data/

Wang, Y., Hong, W., Wu, C. *et al.* Application of landscape ecology to the research on wetlands. *Journal of Forestry Research* **19,** 164 (2008). https://doi.org/10.1007/s11676-008-0029-0

Xie, Y., Sha, Z., & Yu, M. (2008). Remote sensing imagery in vegetation mapping: a review. *Journal of Plant Ecology*, *1*(1), 9–23. http://doi.org/10.1093/jpe/rtm005

Yan, J., Zhou, W., Han, L., & Qian, Y. (2018). Mapping vegetation functional types in urban areas with WorldView-2 imagery: Integrating object-based classification with phenology. *Urban Forestry & Urban Greening*, 31 (1) 230-240 http://doi.org/10.1016/j.ufug.2018.01.021